



Open charm measurements
with new Vertex Detector
at NA61/SHINE experiment
at CERN SPS

Anastasia Merzlaya
Jagiellonian University

Outline

- Introduction;
- Open charm measurements motivation;
- NA61/SHINE experiment at CERN SPS;
- Vertex Detector;
- Track reconstruction in Vertex Detector;
- Data taking results;
- Summary & plans.

Introduction: the Standard Model

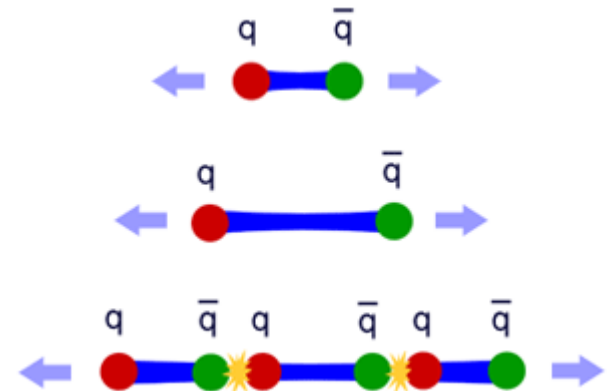
The **Standard Model** is the quantum field theory of elementary particles and interactions between them.

- The Standard Model includes 12 elementary particles of spin $\frac{1}{2}$ - **fermions**. Each fermion has a corresponding antiparticle.
- The fermions of the Standard Model are classified according to how they interact. There are six **quarks** (up, down, charm, strange, top, bottom), and six **leptons**.
- In the Standard Model, gauge bosons are defined as force carriers that mediate the strong (**gluons**), weak (**W^+ , W^- , and Z** gauge bosons), and electromagnetic (**photons**) fundamental interactions.
- The Higgs boson plays a unique role in the Standard Model, by explaining why the other elementary particles, except the photon and gluon, are massive.

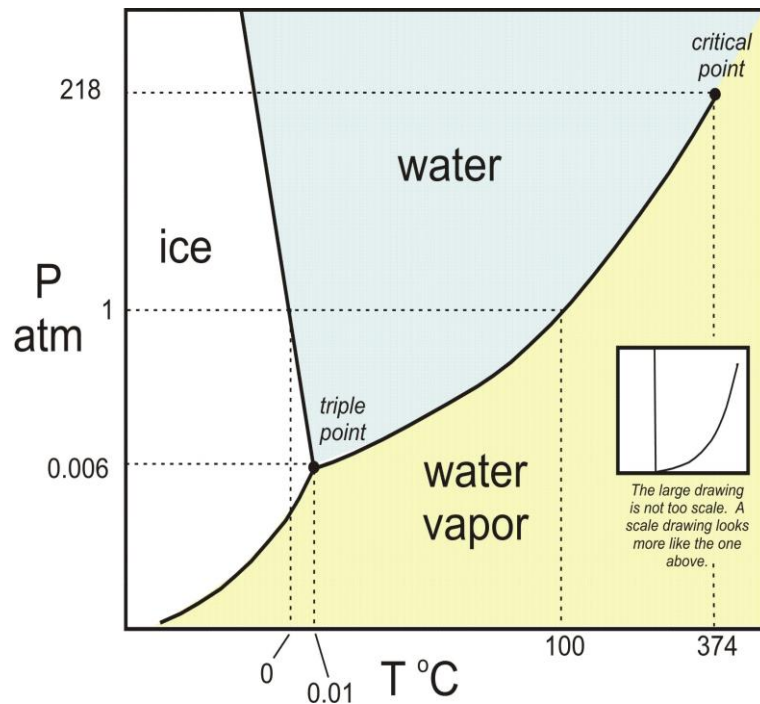
mass →	$\approx 2.3 \text{ MeV}/c^2$	$\approx 1.275 \text{ GeV}/c^2$	$\approx 173.07 \text{ GeV}/c^2$	0	$\approx 126 \text{ GeV}/c^2$
charge →	$\frac{2}{3}$	$\frac{2}{3}$	$\frac{2}{3}$	0	0
spin →	$\frac{1}{2}$	$\frac{1}{2}$	$\frac{1}{2}$	1	0
	u up	c charm	t top	g gluon	H Higgs boson
QUARKS	$\approx 4.8 \text{ MeV}/c^2$	$\approx 95 \text{ MeV}/c^2$	$\approx 4.18 \text{ GeV}/c^2$	0	
	$-\frac{1}{3}$	$-\frac{1}{3}$	$-\frac{1}{3}$	0	
	$\frac{1}{2}$	$\frac{1}{2}$	$\frac{1}{2}$	1	
	d down	s strange	b bottom	γ photon	
	$0.511 \text{ MeV}/c^2$	$105.7 \text{ MeV}/c^2$	$1.777 \text{ GeV}/c^2$	$91.2 \text{ GeV}/c^2$	
	-1	-1	-1	0	
	$\frac{1}{2}$	$\frac{1}{2}$	$\frac{1}{2}$	1	
	e electron	μ muon	τ tau	Z Z boson	
LEPTONS	$< 2.2 \text{ eV}/c^2$	$< 0.17 \text{ MeV}/c^2$	$< 15.5 \text{ MeV}/c^2$	$80.4 \text{ GeV}/c^2$	
	0	0	0	± 1	
	$\frac{1}{2}$	$\frac{1}{2}$	$\frac{1}{2}$	1	
	ν_e electron neutrino	ν_μ muon neutrino	ν_τ tau neutrino	W W boson	
				GAUGE BOSONS	

Quantum Chromodynamics (QCD)

- Quantum Chromodynamics (QCD) is the theory of strong interactions which fundamentally describes hadronic matter.
- It assumes the existence of **color** – additional state of freedom.
- **Color confinement**: quarks and gluons can not be directly observed due to their color charge and are always bound within hadrons;
- **Asymptotic freedom**: attraction between quarks is weak at short distances and with increasing distance that attraction becomes stronger.

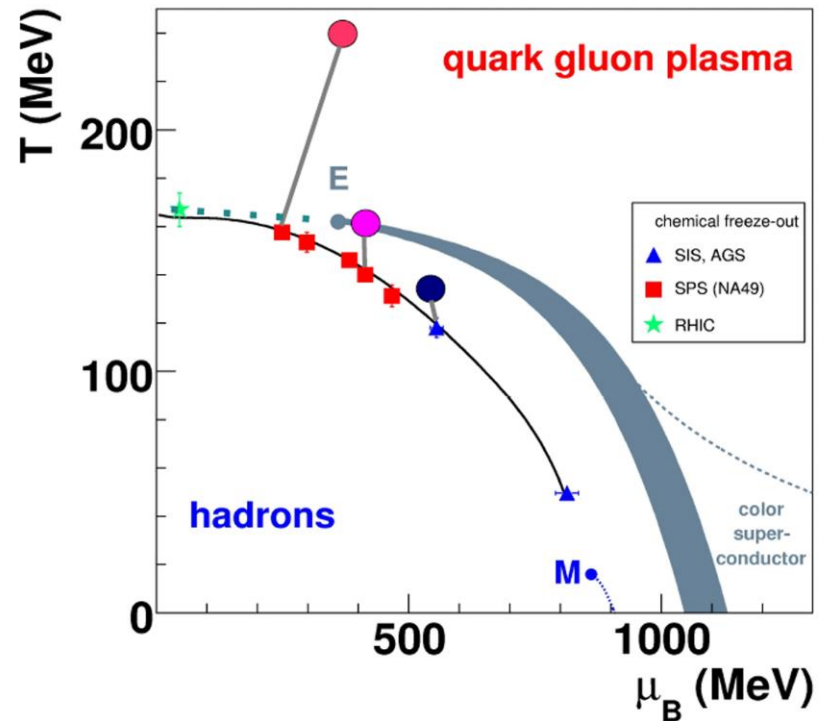
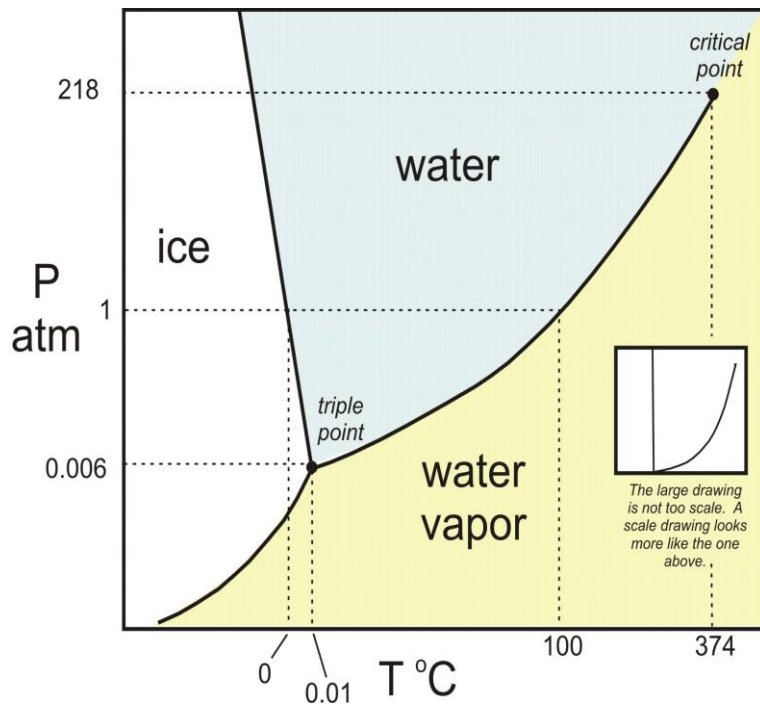


Phase diagram of H₂O



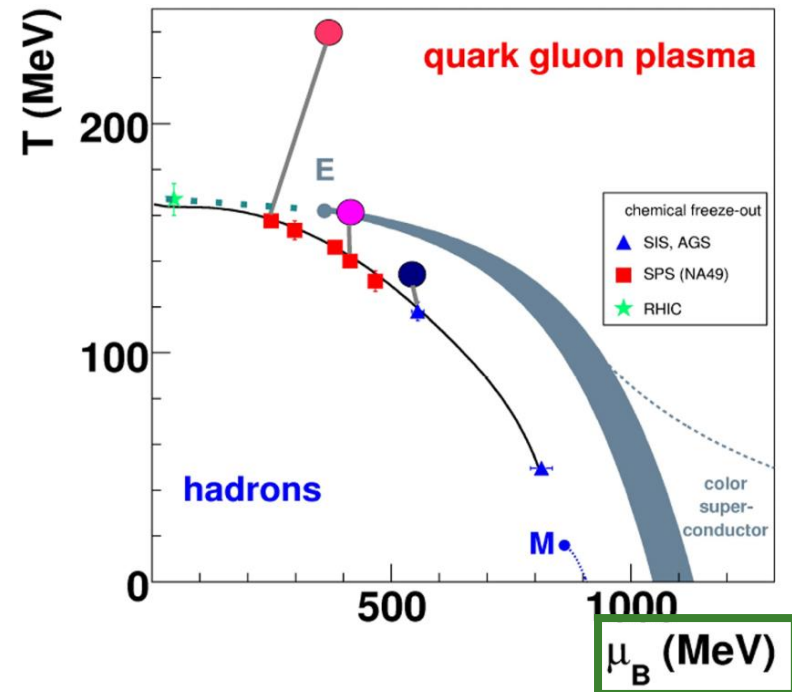
- The lines mark the various coexistence curves $P(T)$ where two phases are in equilibrium;
- A phase transition such as melting or boiling is observed when moving along a path in the (T, P) plane which intersects such curves.
- **Triple point:** all three phases coexist;
- **Critical point:** the meniscus separating liquid from vapor disappears, and the two fluid phases become indistinguishable;
 - For $T < T_c$ the transition between liquid and vapor is first order;
 - At the critical point the transition becomes second order.

Phase diagram of strongly interacting matter



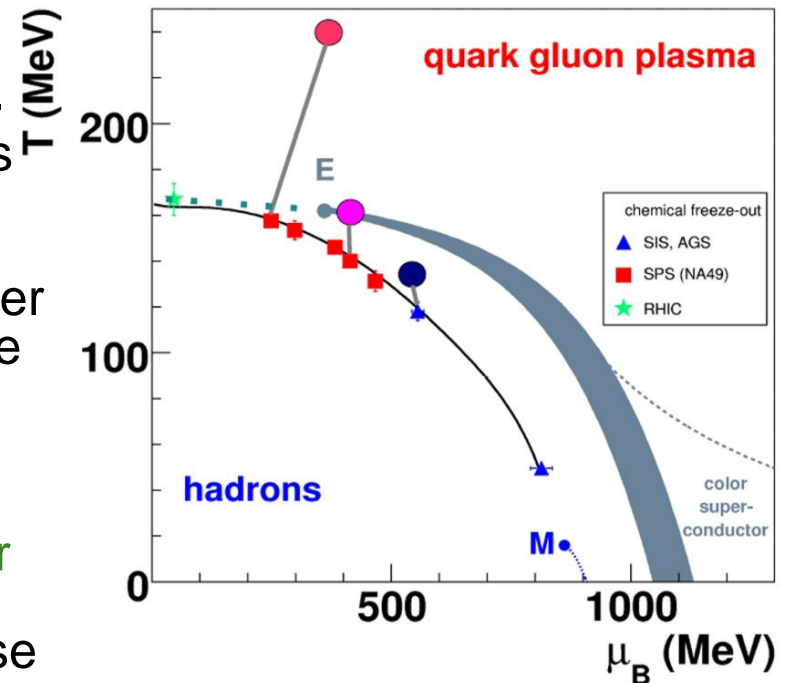
Phase diagram of strongly interacting matter

- The μ_B variable is the **baryon chemical potential**;
- It is the energy needed to add or remove one baryon from the system;
- μ_B expresses the asymmetry between baryons and anti-baryons. The higher value of μ_B , the bigger disproportion between produced matter and anti-matter;
- In an ordinary nuclear matter the baryon chemical potential is approximately equal to the mass of the nucleon $\mu_B \approx m_N = 940 \text{ MeV}$.



Phase diagram of strongly interacting matter

- For lower values of temperature and baryon chemical potential the main phase is **Hadron Gas**;
- With higher temperature the system is in a state of **Quark-Gluon Plasma**.
- Lower temperatures and high values of μ_B exist in neutron stars;
- For $\mu_B \rightarrow 0$ the change of the character of phase transition is predicted to the **smooth cross-over** with the continuous change of physical parameters;
- For higher values of μ_B the **first order phase transition** is expected (grey band), the line of the first-order phase transition ends with the so-called **critical point**.



Heavy-ion collisions

- In a laboratory, deconfined matter can be created in **relativistic heavy-ion collisions**;
- Since the medium lives only for a short time after the collision, the effective tool for studying properties of the medium is measurement of particles that are created in the collision and interact with the medium, as probes of the medium;
- So-called **hard probes** are particles produced in the hard scattering at the initial stage of the collisions;
- Heavy quarks like charm are mainly produced by parton-parton collisions in the early stage of the collisions.
These quarks propagate through and interact with the medium.

Charm particles

- Charm quarks

c charm quark

\bar{c} anti-charm quark

- Open charm particles

D^0
 $c\bar{u}$

\bar{D}^0
 $\bar{c}u$

D^+
 $c\bar{d}$

D^-
 $\bar{c}d$

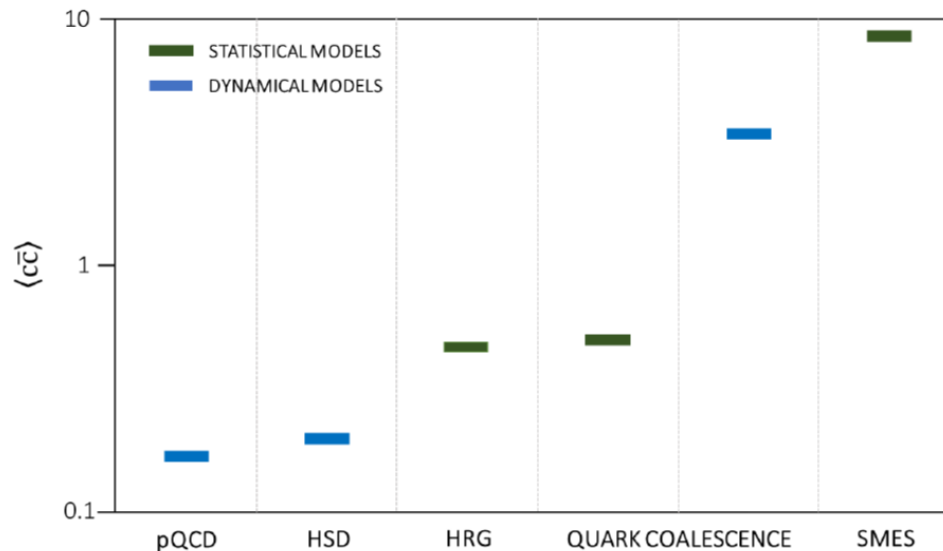
.....

- Closed charm particles

J/ψ
 $c\bar{c}$

Models of charm production

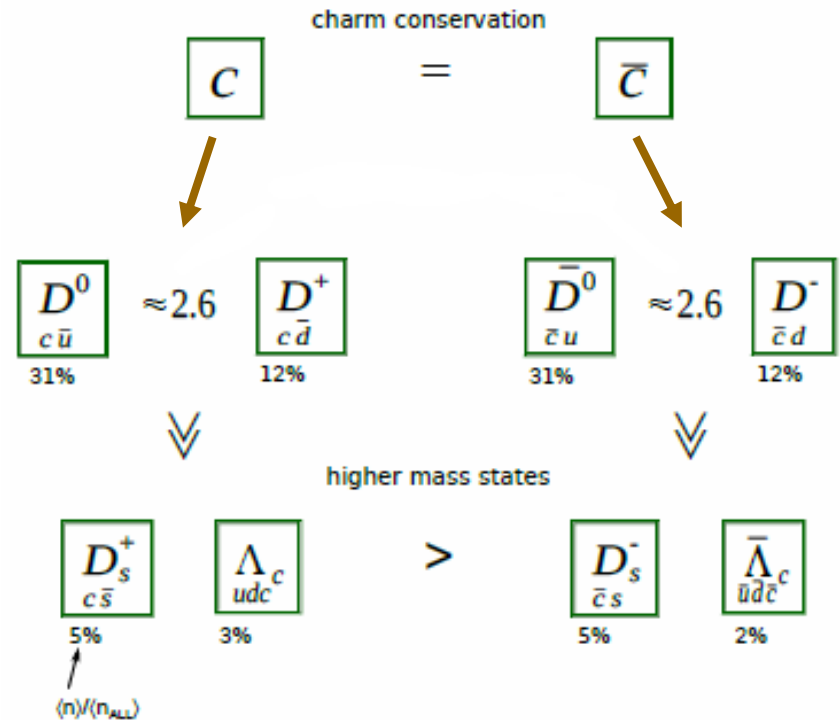
- Predictions of charm yield
 - Dynamical approach;
 - Statistical approach;
 - Results for produced $\langle c\bar{c} \rangle$ pairs differ by up to two orders of magnitude for central Pb+Pb collisions at top SPS energy (150A GeV/c);
- Therefore, obtaining precise data on $\langle c\bar{c} \rangle$ is expected to allow to narrow the spectrum of viable theoretical models and thus learn about the charm quark and hadron production mechanisms.



pQCD
Gavai *et al.* IJMP A 10 2999.
Braun-Munzinger, J. Stachel,
PL B 490, 196.
HSD
Linnyk, Bratkovskaya, Cassing,
IJMP E17 1367
HRG, Quark Coalesc. Stat.
Gorenstein, Kostyuk, Stoecker,
Greiner, PL B 509, 277.
Quark Coalesc. Dyn.
Levai, Biro, Csizmadia, Csorgo,
Zimanyi, JP G 27, 703
SMES
Gazdzicki, Gorenstein, APP B30,
2705.

Measurements of $\langle c\bar{c} \rangle$

- Good estimate of $\langle c\bar{c} \rangle$ can be obtained measuring yields of D^0 , D^+ and their antiparticles since they carry $\sim 85\%$ of the total produced charm;

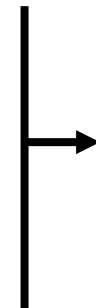


Total charm distribution over different charm hadrons according to PHSD model 0-20% Pb+Pb at 150A GeV/c

Charm particles as a signal of deconfinement

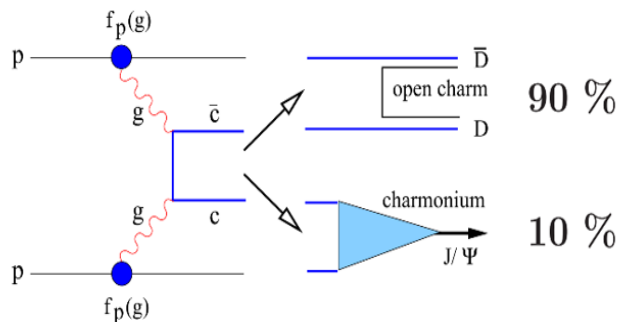
- The production of charm is expected to be different in confined and deconfined matter.

- Confined matter:
lightest charm carrier – D meson;
production of $\langle D\bar{D} \rangle$ pair $\sim 3.7\text{GeV}$;
- Deconfined matter:
charm carrier – (anti-)charm quark;
production of $\langle c\bar{c} \rangle$ pair $\sim 2.6\text{GeV}$.

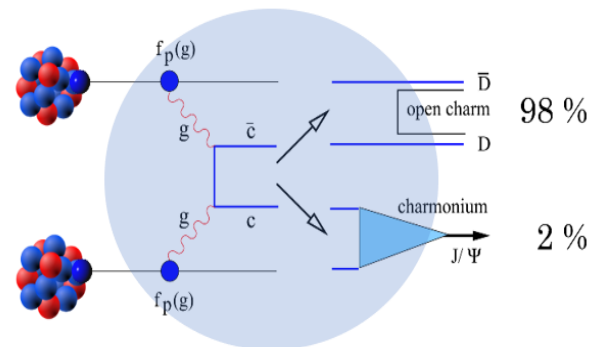


More abundant charm production is expected in deconfined than in confined matter;
 → change of collision energy dependence of may be a signal of onset of deconfinement

vacuum

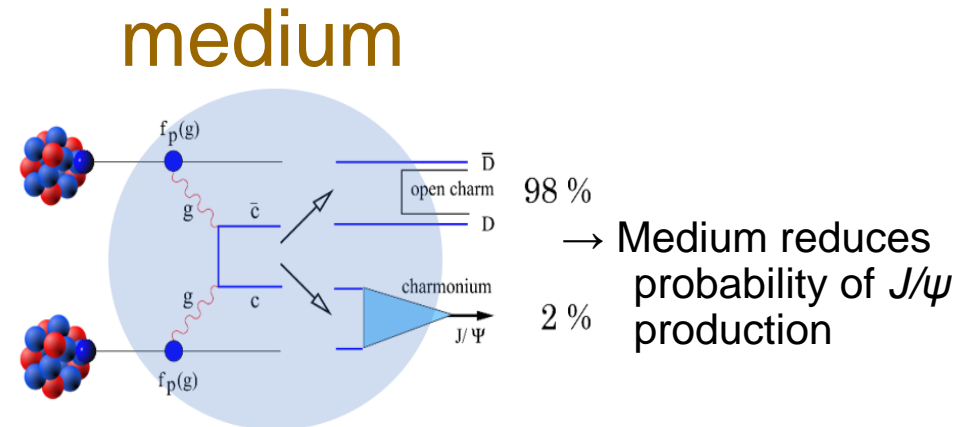
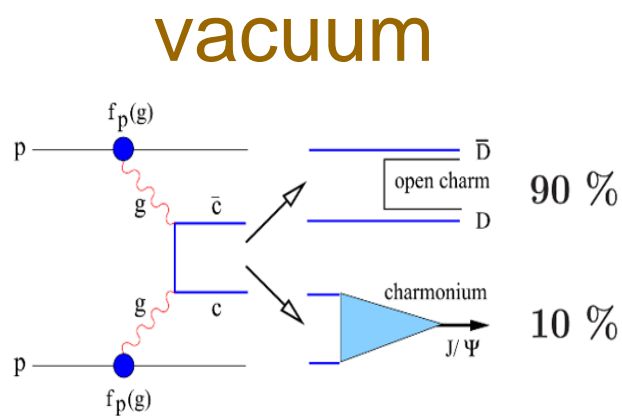


medium



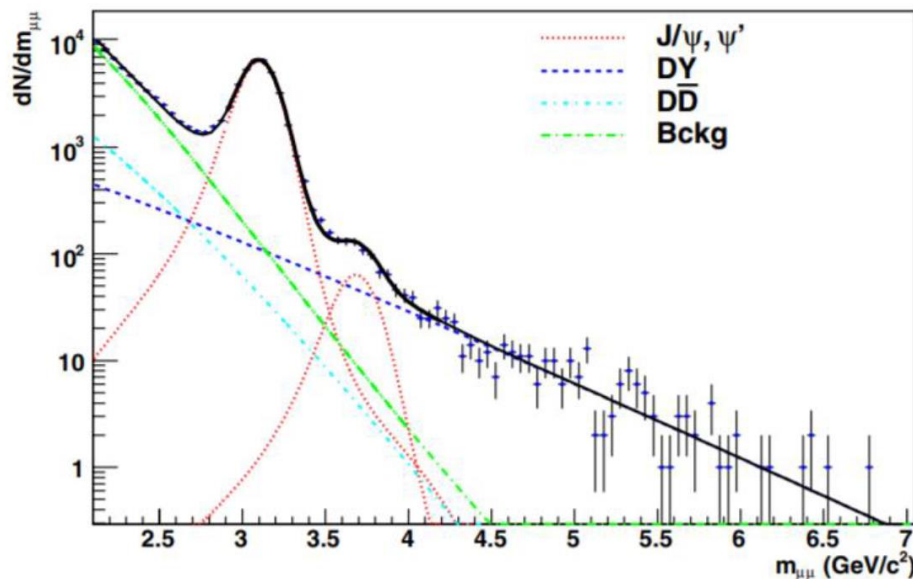
Charm particles as a signal of deconfinement

- The production of charm is expected to be different in confined and deconfined matter.
- For deconfined and confined matter we expect to have different ratio of J/ψ and open charm production;
- To provide information of influence of final state interaction on J/ψ yield one needs to provide measurements of both closed and open charm production.



Charm measurements at SPS

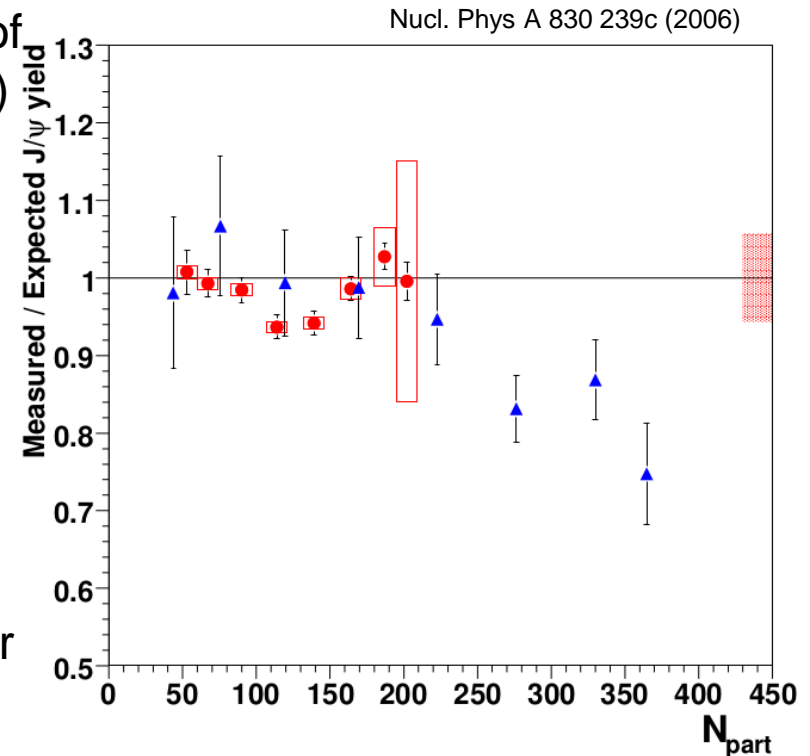
- At the CERN SPS precise $\langle J/\psi \rangle$ data was provided by the NA38, NA50, and NA60 experiments, while $\langle c\bar{c} \rangle$ data is not available at the CERN SPS energies;
- These experiments measured $\langle J/\psi \rangle$ via study of dimuon production in In+In and Pb+Pb at SPS energies;



- From the measured dimuon invariant mass structure, contributions from J/ψ , ψ' and open charm were separated from the background;

Abnormal J/ψ suppression

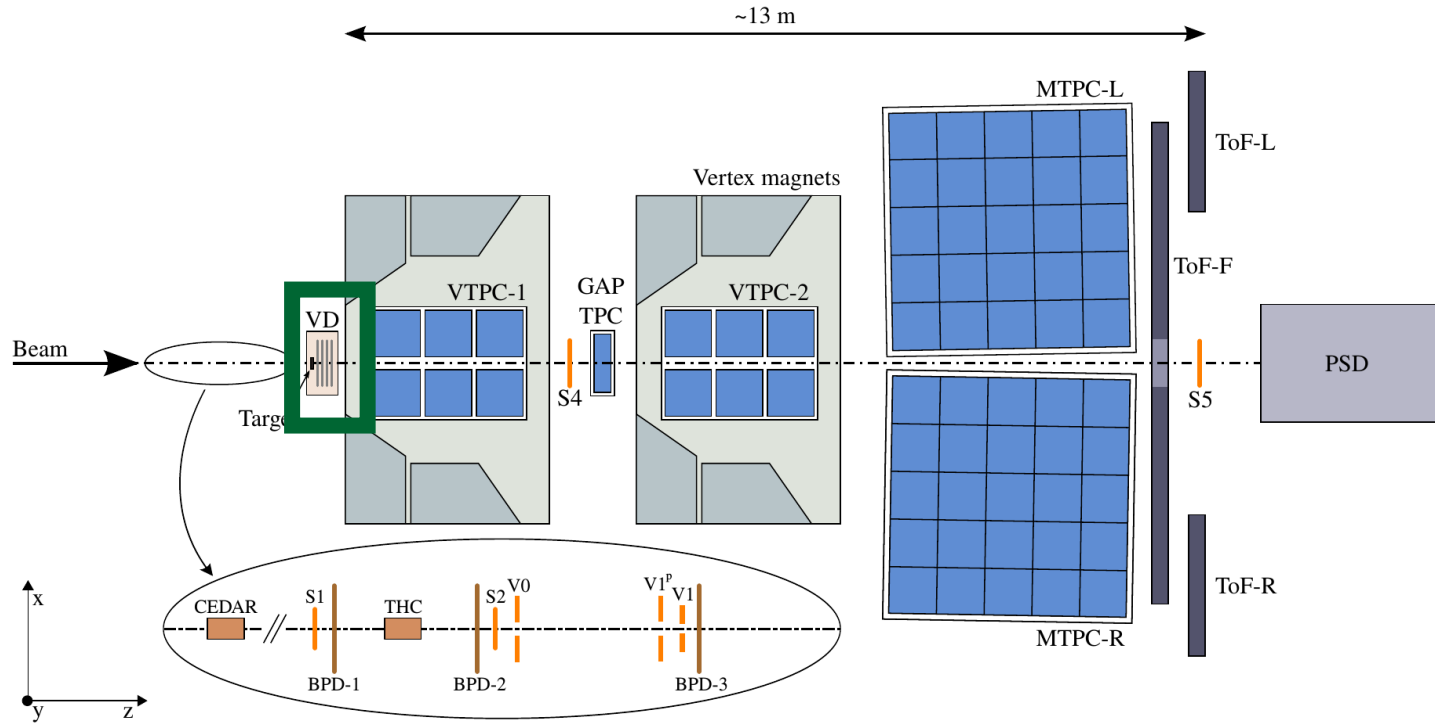
- NA60 experiment measured the production of J/ψ in In+In (red dots) and Pb+Pb (blue dots) collisions;
 - For lower number of participants the yields are consistent with the theoretical estimations;
 - However, at $N_{\text{part}} \sim 200$ the result shows significant drop, which is known as the effect of **anomalous J/ψ suppression**;
 - It was initially attributed to onset of QGP formation in nuclear collisions, however other explanations have also been proposed.
-
- To verify observed signature of QGP formation one needs to obtain information on total balance of charm.
 - This can be achieved by measurement of **charm production in all channels**.



Open charm measurements motivation

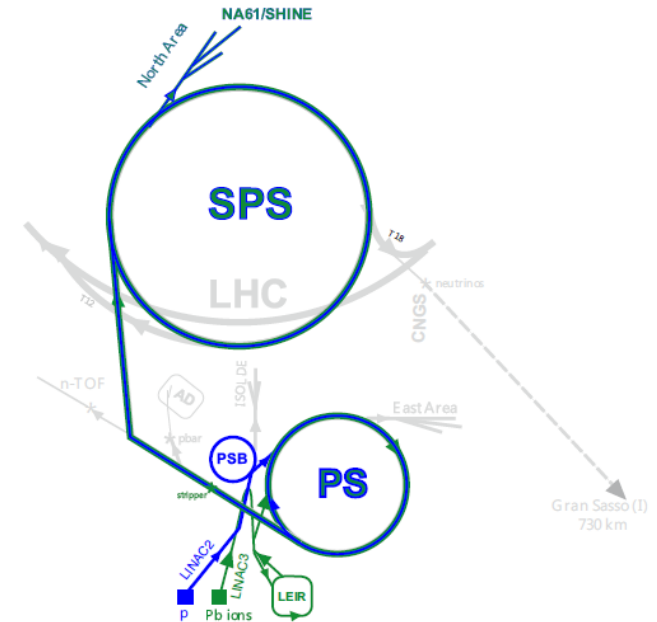
- Charm measurements:
 - What is the mechanism of open charm production?
 - How does the onset of deconfinement impact open charm production?
 - How does the formation of quark-gluon plasma impact J/ψ production?
- To answer these questions **mean number of charm quark pairs** $\langle c\bar{c} \rangle$ produced in the full phase space in A+A collisions has to be known.
- Up to now corresponding experimental data does not exist;
- → One need direct **measurements of open charm yields**.

The NA61/SHINE experiment



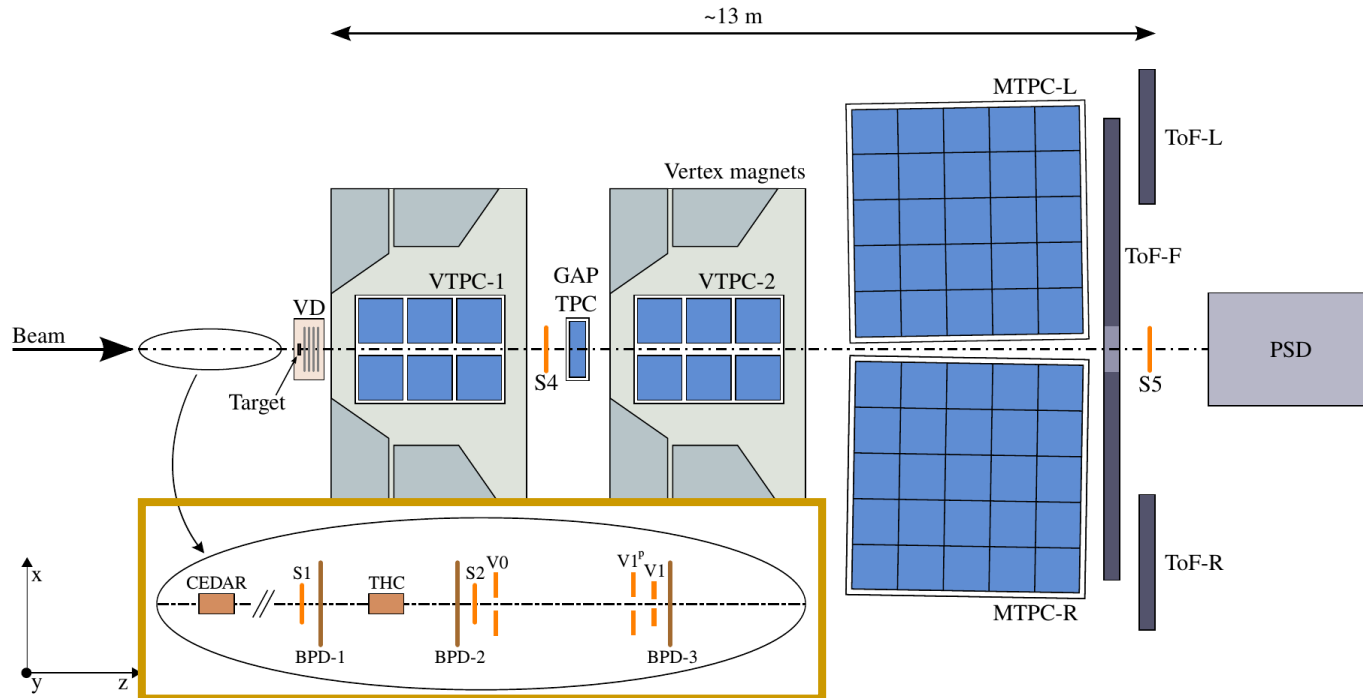
- The heavy-ion programme of the NA61/SHINE experiment at CERN SPS was being expanded to allow precise measurements of exotic particles with short lifetime, such as D-mesons;
- → NA61/SHINE experiment was upgraded with the new **Small Acceptance Vertex Detector (SAVD)**.

The NA61/SHINE experiment



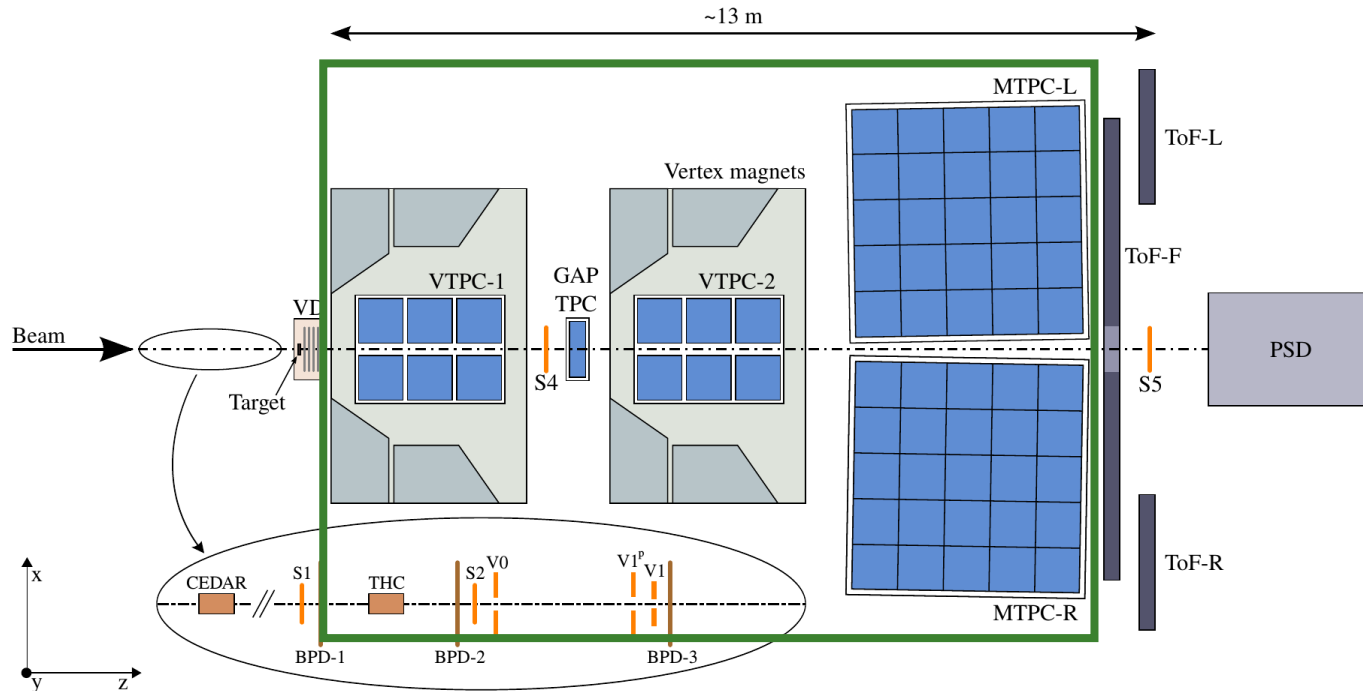
- Hadrons (π , K, p) and ions (Be, Ar, Xe, Pb)
- $P_{\text{beam}} = 13A-158A(400)\text{GeV}/c$
- $\sqrt{s} = 5.1-17.3 (27.4)\text{GeV}/c$

The NA61/SHINE experiment



- Beam detectors
 - Position
 - Charge
 - Time
- of beam particles

The NA61/SHINE experiment



Beam detectors

- Position
- Charge
- Time

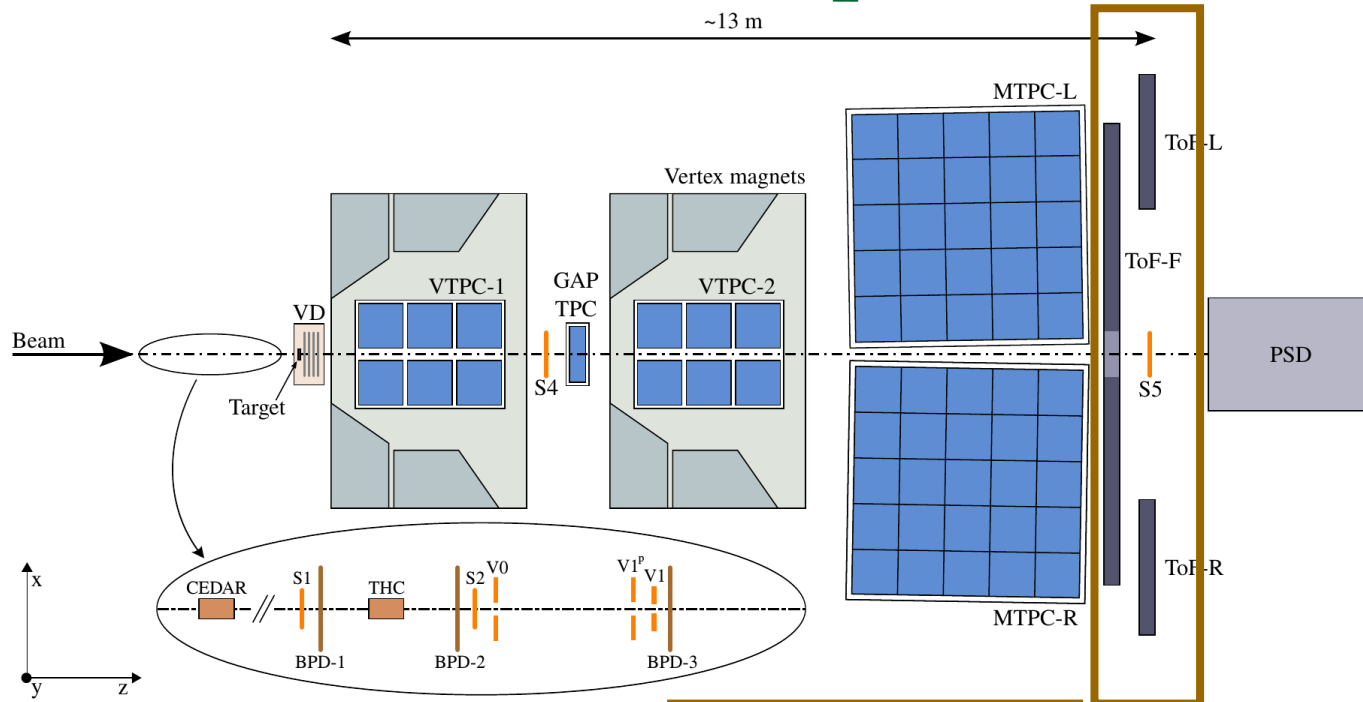
of beam particles

TPCs

- Momentum
- Charge
- PID (dE/dx)

of produced particles

The NA61/SHINE experiment



Beam detectors

- ❑ Position
- ❑ Charge
- ❑ Time

of beam particles

TPCs

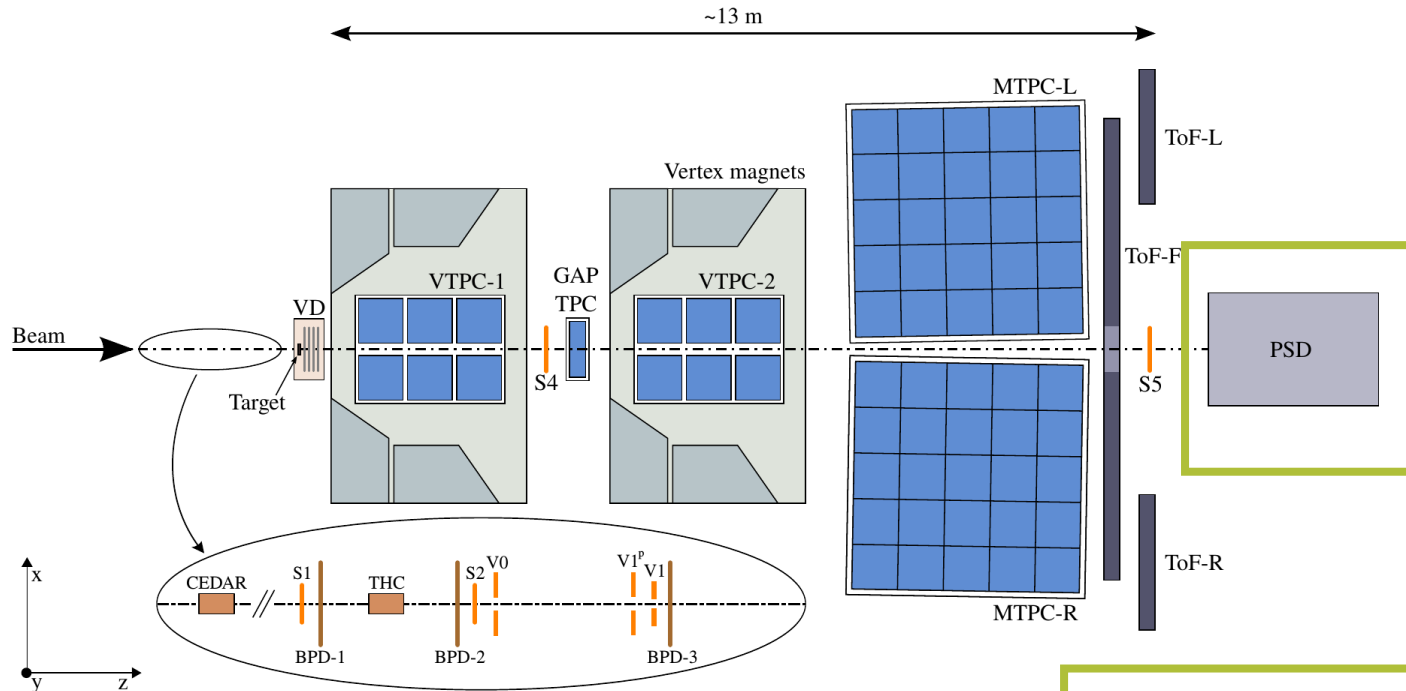
- ❑ Momentum
- ❑ Charge
- ❑ PID (dE/dx)

of produced particles

ToF

- ❑ PID (mass)

The NA61/SHINE experiment



Beam detectors

- Position
- Charge
- Time

of beam particles

TPCs

- Momentum
- Charge
- PID (dE/dx)

of produced particles

ToF

- PID (mass)

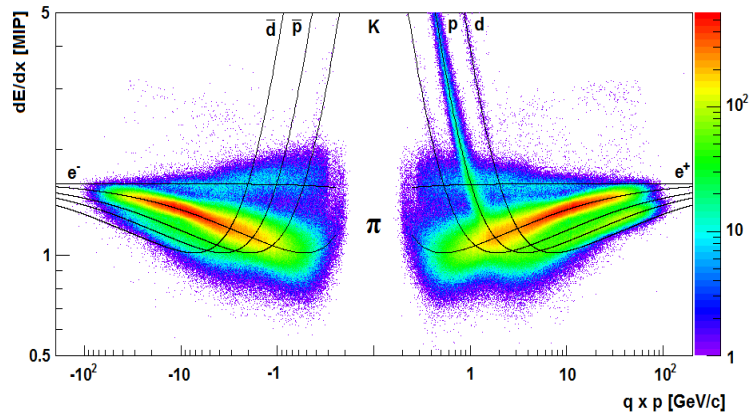
PSD calorimeter

- energy

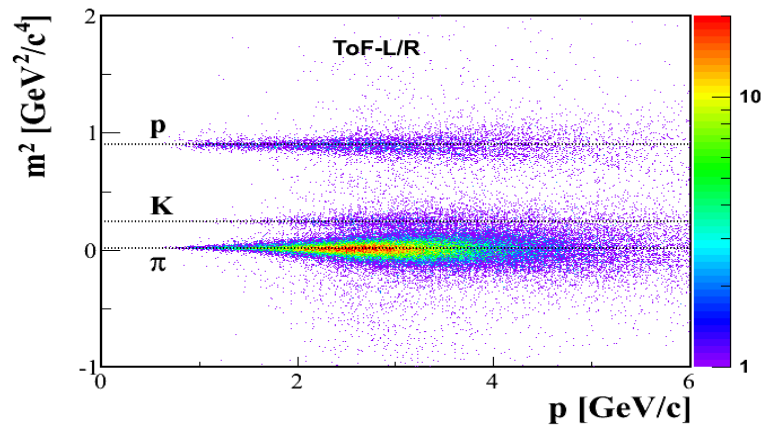
of projectile
spectators

TPC-ToF measurements

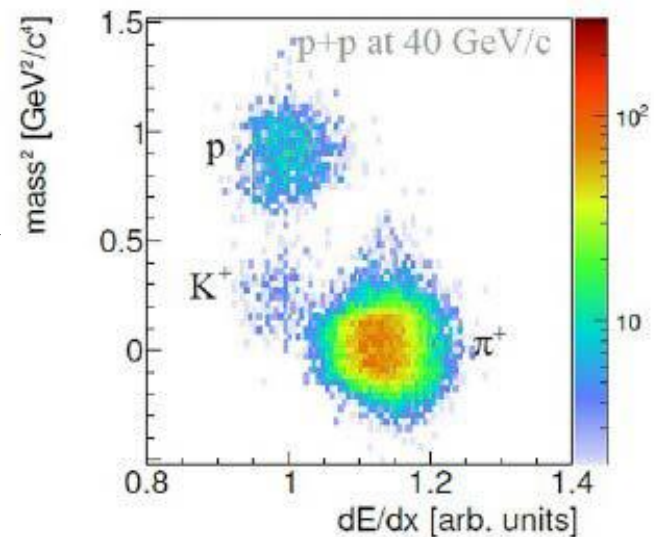
TPC



ToF



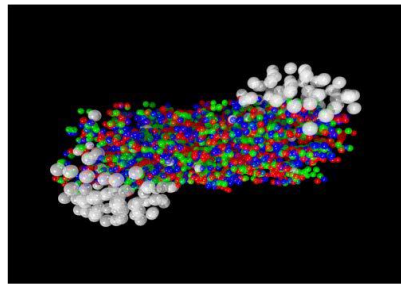
- Combining TPC and ToF information about track one gets good PID separation.



Projectile Spectator Detector (PSD)

- PSD measures the energy of projectile spectators.
- It allows to determine the number of projectile nucleons which participated in a collision with a precision of about one nucleon
→ Gives the centrality of collisions

$$N_p = A - \frac{E_S}{E_A}$$



- N_p – number of participants
- A – mass number of ion
- E_A – beam energy per nucleon
- E_S – energy carried by the non-interacting nucleons (projectile spectators) measured by PSD

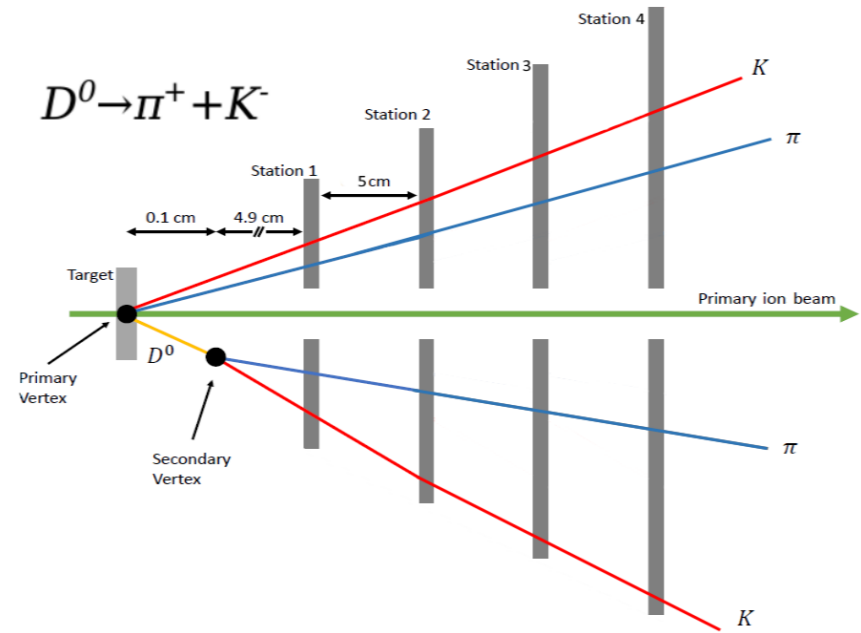


Open charm measurements in the NA61 / SHINE experiment

Programme for open charm measurements

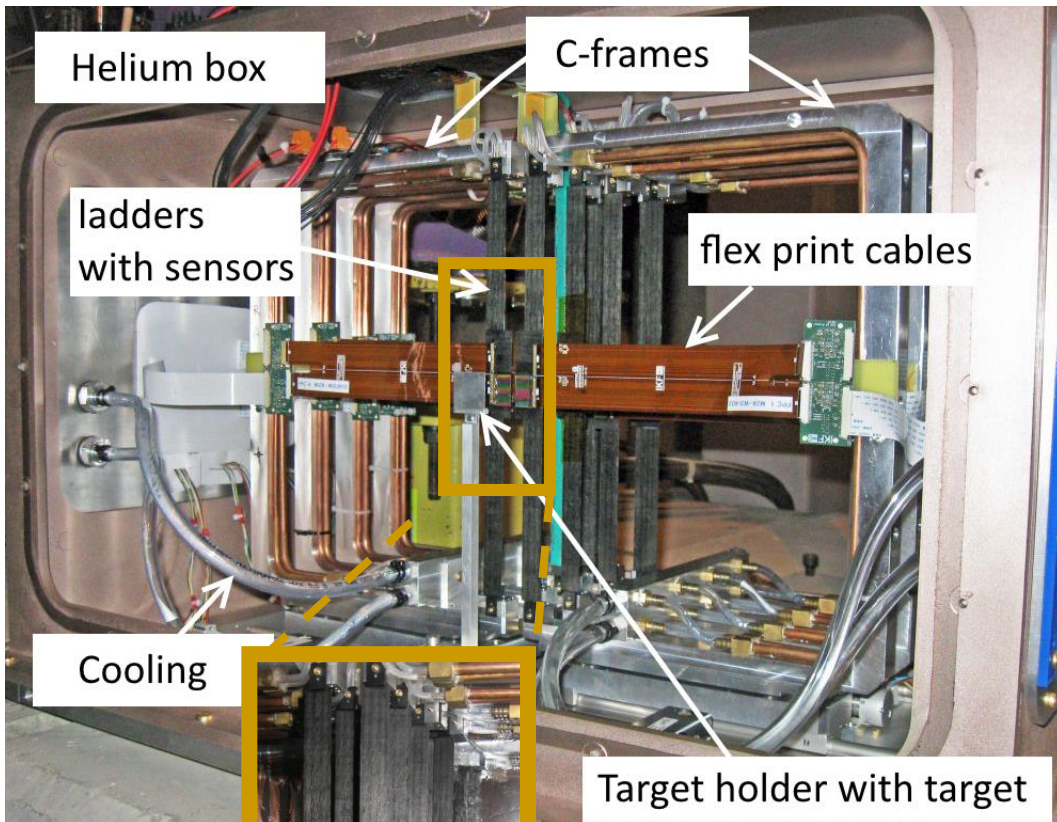
- The low yields of charmed particles → require precise tracking and low material budget close to the primary vertex;
- The short mean life-time of D mesons → rather small distance between the decay vertices of D mesons and the primary vertex.

→ Vertex Detector project based on CMOS pixel detectors.

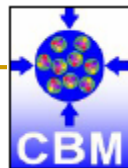
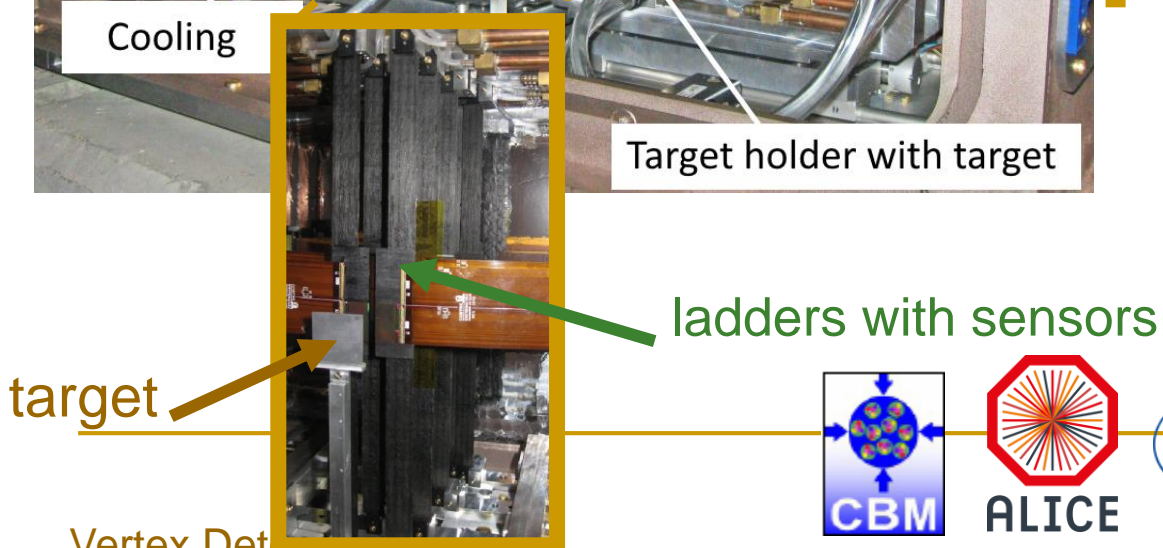


Meson	Decay channel	$c\tau$	Branching ratio
D^0	$D^0 \rightarrow K^- + \pi^+$	$122.9 \mu\text{m}$	$(3.91 \pm 0.05)\%$
D^0	$D^0 \rightarrow K^- + \pi^+ + \pi^+ + \pi^-$	$122.9 \mu\text{m}$	$(8.14 \pm 0.20)\%$
D^+	$D^+ \rightarrow K^- + \pi^+ + \pi^+$	$311.8 \mu\text{m}$	$(9.2 \pm 0.25)\%$
D_s^+	$D_s^+ \rightarrow K^+ + K^- + \pi^+$	$149.9 \mu\text{m}$	$(5.50 \pm 0.28)\%$
D^{*+}	$D^{*+} \rightarrow D^0 + \pi^+$...	$(61.9 \pm 2.9)\%$

Vertex Detector

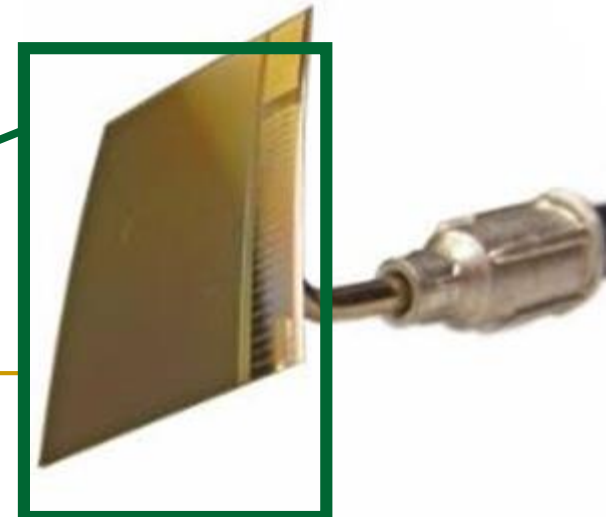
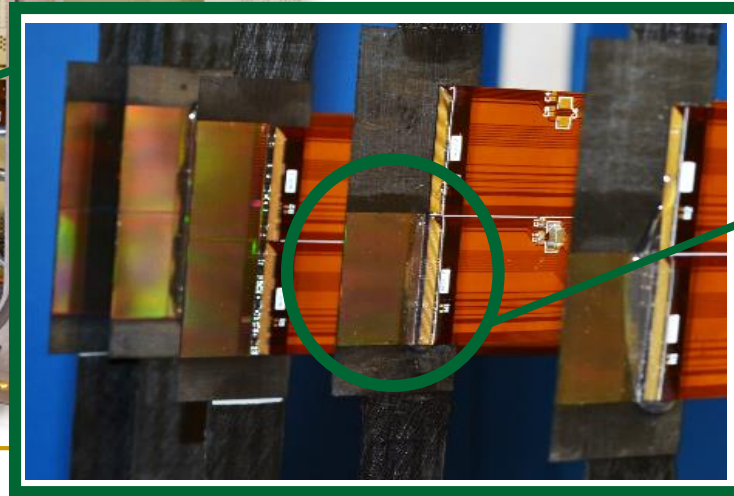
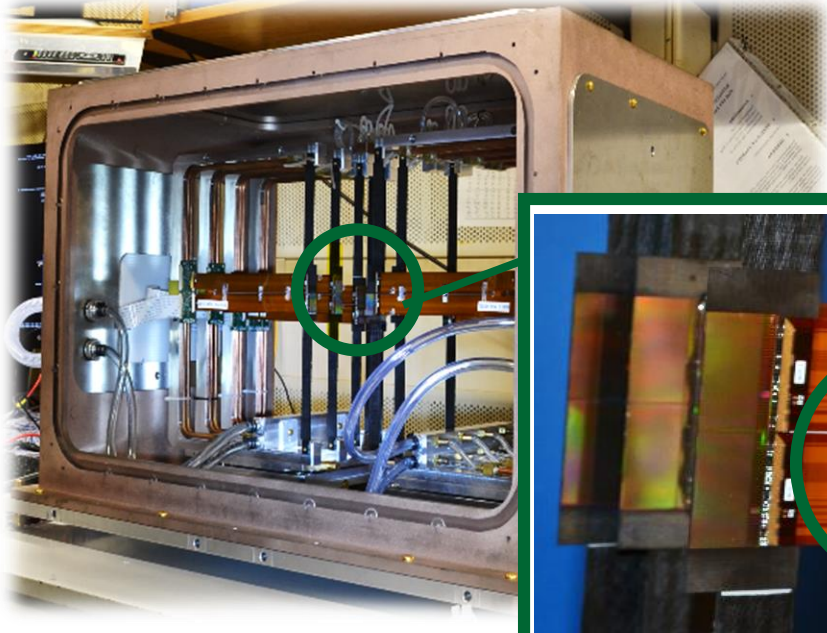


- Main purpose of the **Vertex Detector** is the improvement of track resolution near the interaction point to allow reconstruction of secondary vertices;
- **SAVD** is positioned between the target and the VTPC-1;
- Four planes of coordinate-sensitive detectors are located at 5, 10, 15 and 20 cm distance from the target.



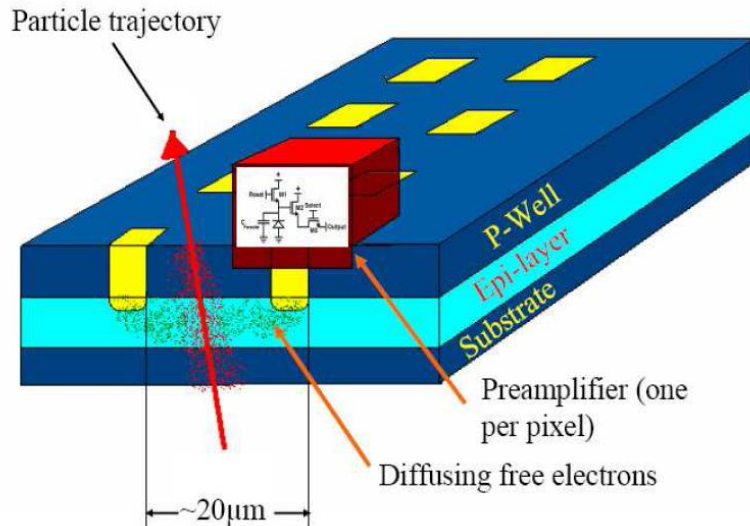
Si pixel detectors

- High position resolution MIMOSA-26 sensors are CMOS **Monolithic Active Pixel Sensor** (MAPS) and have very low material budget → have been chosen as the basic detection element of the Vertex Detector stations.
- 1152x576 pixels of $18.4 \times 18.4 \mu\text{m}^2$;
- 3.5 μm resolution;
- Readout time: 115.2 μs ;
- 50 μm thin.



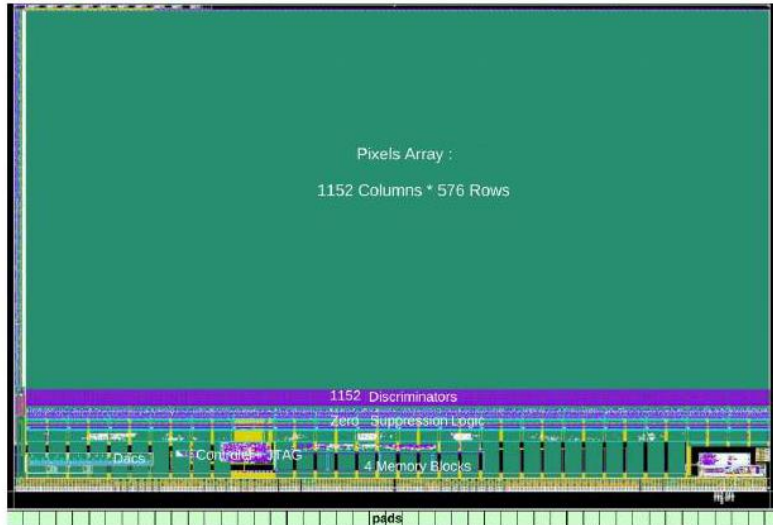
Vertex Detector

Si pixel detectors



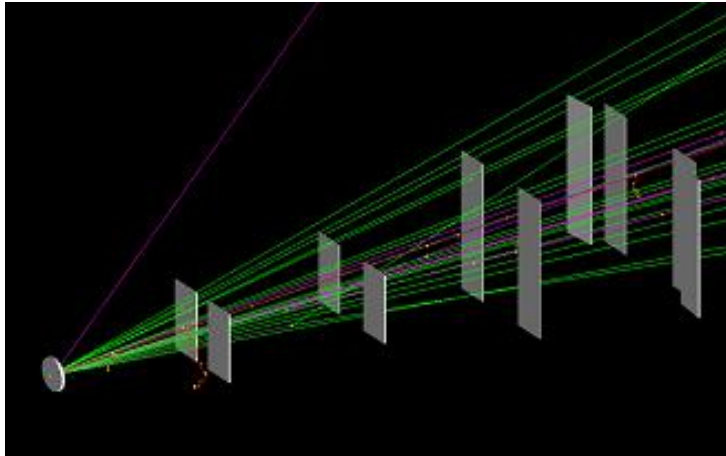
- Passing through sensor particle creates electron-hole pairs;
- The electric field separates these produced charges, and thus avoids recombination;
- Electrons drift toward the anode, while holes drift to the cathode;
- This collected charge produces a current pulse on the electrode, whose integral equals the total charge generated by the incident particle.
- If the collected charge above threshold pixel is “fired” → have a hit.

VD readout

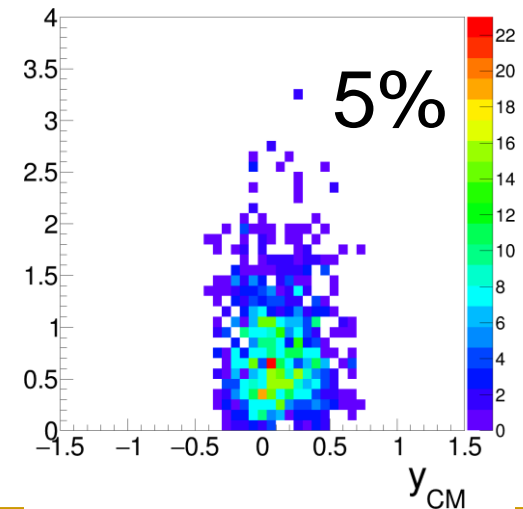
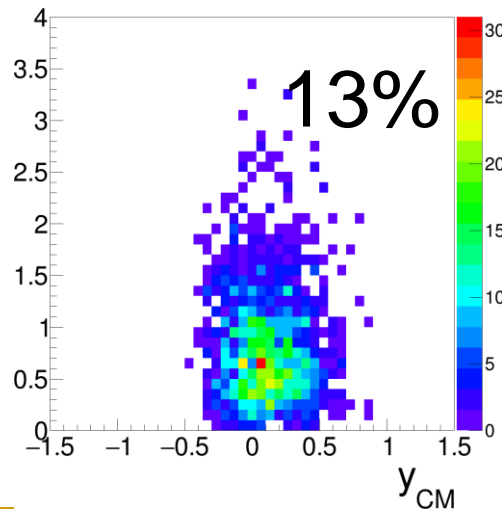
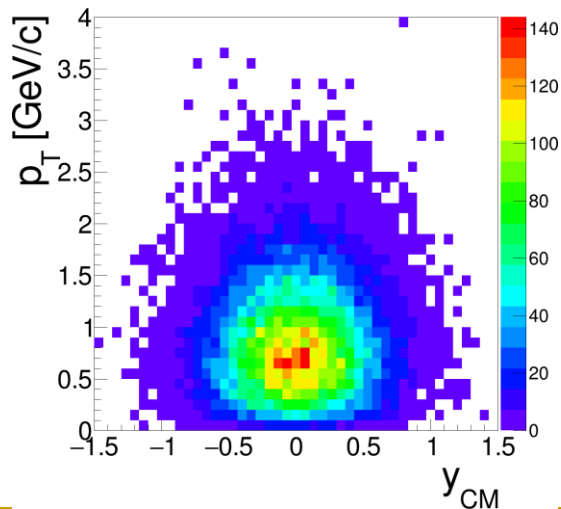


- An array of 1152x576 pixels with the readout and processing electronics located at the periphery of the chip;
- Every pixel in the array is connected to an analogue output and can be accessed by selecting the row line by means of two shift registers;
- The pixels are read sequentially and will be referred to as serial readout;
- Once all pixels in the matrix have been read out, the process re-starts from the first pixel;
- In general, the time resolution is equal to the readout time of a frame. A typical readout time for the serial readout approach is 115.2 μ s.

SAVD: acceptance



- Estimation of SAVD acceptance for D^0 mesons in $D^0 \rightarrow K^- + \pi^+$ with GEANT4 simulation study.



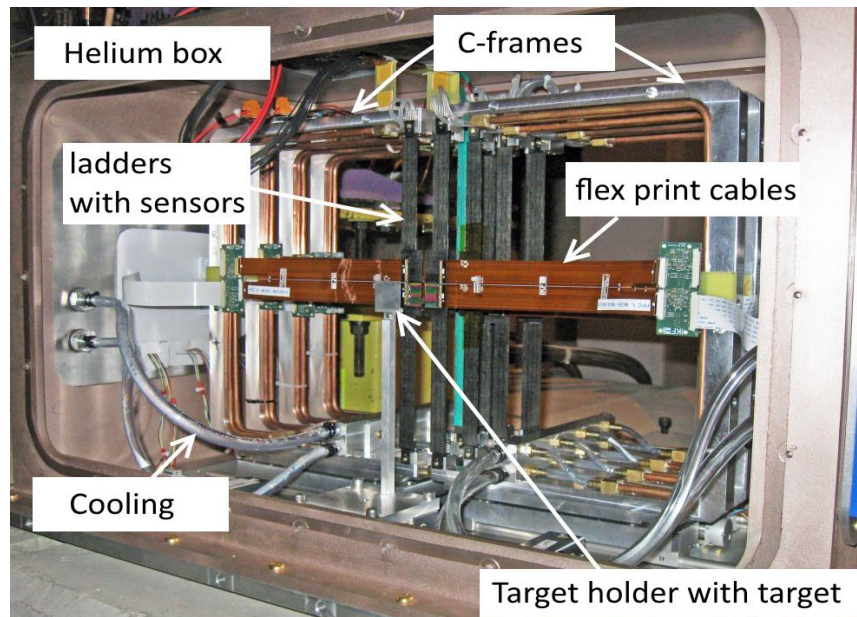
All generated

VD&TPC accepted

Accepted with cuts

SAVD data taking

- **Dec. 2016** Vertex Detector was installed for data taking with the beam of Pb at 150A GeV/c with 1mm Pb target located 50 mm downstream from the first station;
- **Oct.-Dec. 2017** Vertex Detector was installed for data taking with the beam of Xe at 150A, 75A, 40A GeV/c with (1+1+1)mm La target located 50 mm downstream from the first station;
- **Nov.-Dec. 2018** Pb+Pb at 150A GeV/c data taking.

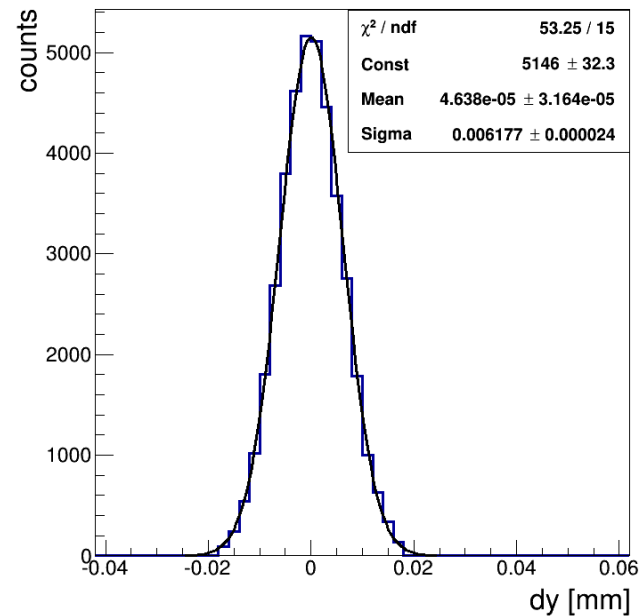
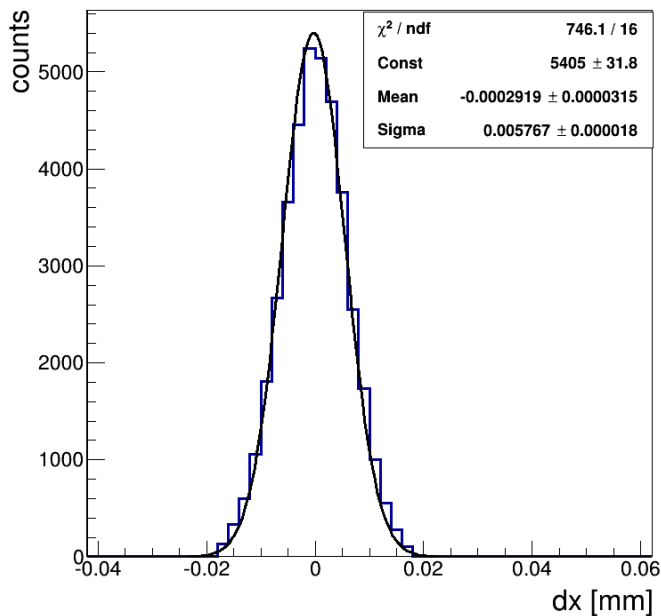


Reconstruction algorithm in SAVD

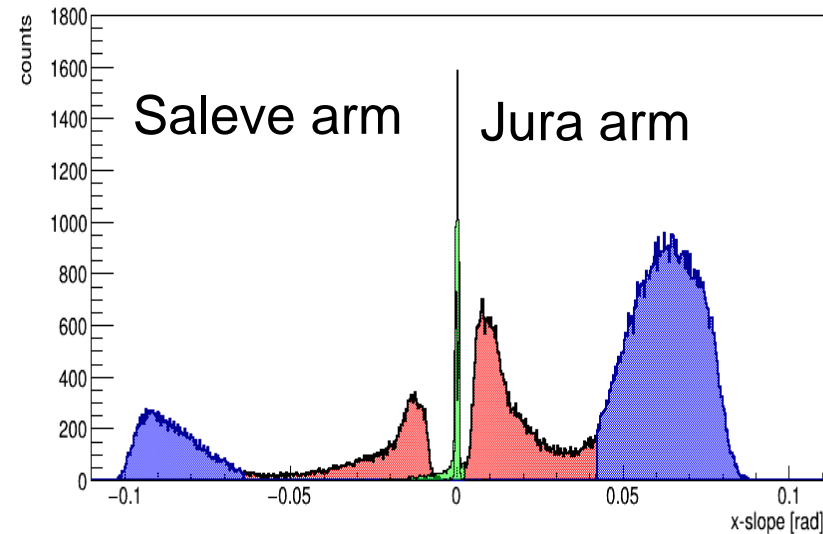
- The SAVD consists of two arms: Jura and Saleve, in which track reconstruction can be done independently;
- The magnetic field in SAVD volume is inhomogeneous ($B_y = 0.13 \div 0.25\text{T}$);
- **Track reconstruction** is done iteratively:
 1. Finding 4-hit tracks by a **combinatorial method** with straight line track model;
 2. Reconstruction of the primary vertex;
 3. Using information about the primary vertex position one can find 3-hit tracks using the **Hough Transform** method;
 4. Fitting tracks with a parabola in (XZ) plane and a straight line in (YZ) plane.
- **Track matching** between VD and TPC is done using the following algorithm: tracks are fitted to the VD primary vertex and then interpolated to other VD stations and the matching clusters are collected;
- Finally, the whole track is refitted using the Kalman Filter.

Spatial sensor resolution

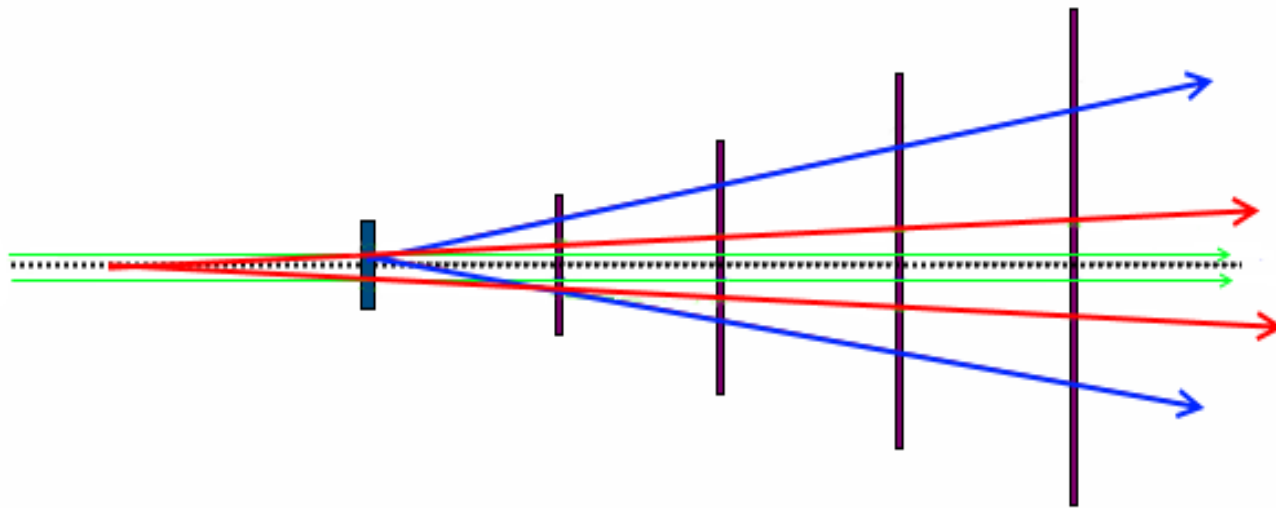
- **Spatial sensor resolution** obtained by looking at residuals between hits and reconstructed tracks for non-field runs is $\sigma_x = 4.7\mu\text{m}$ and $\sigma_y = 5.0\mu\text{m}$.



Angle distribution of the tracks

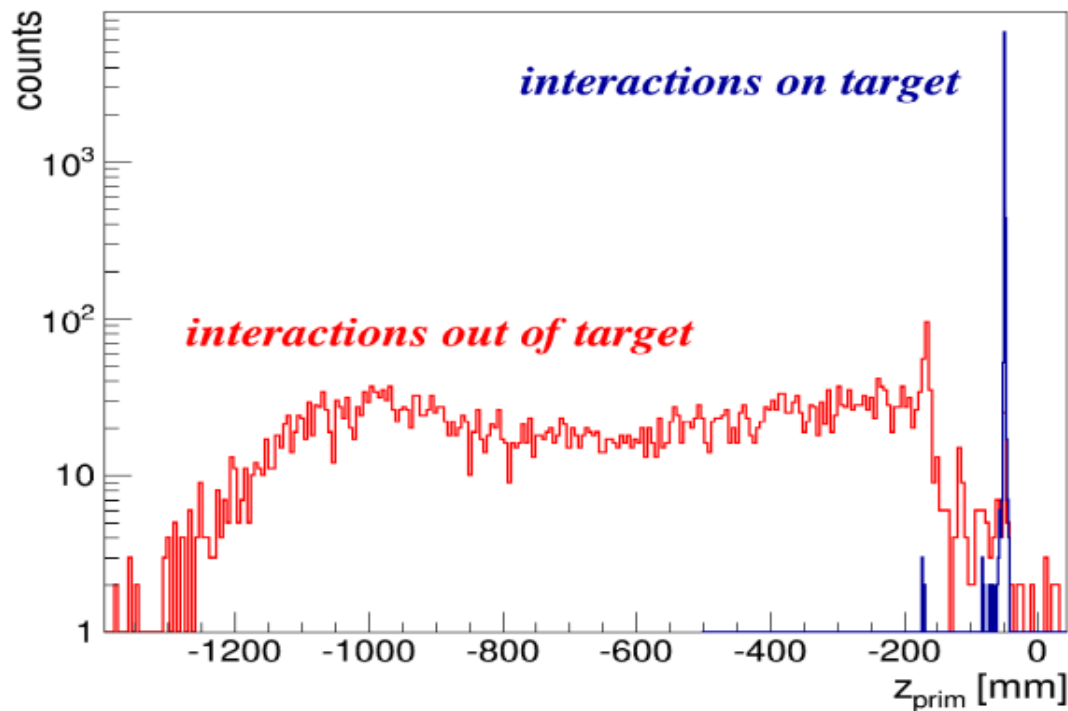
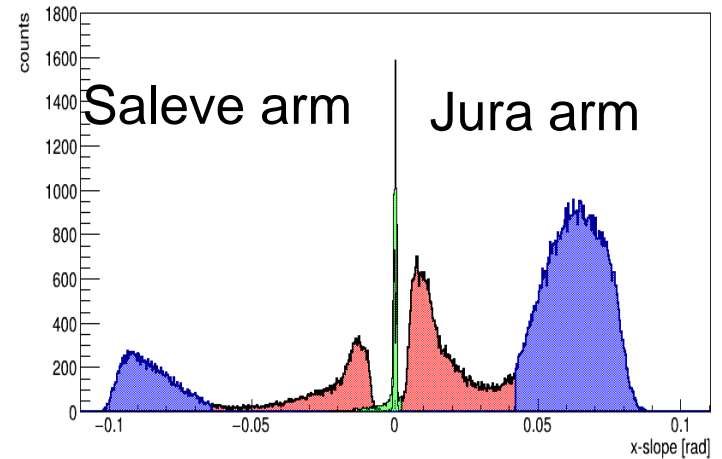


- **Blue:** peaks associated with production on target;
- **Red:** peaks associated with production in the near target region;
- **Green:** narrow peaks associated with far upstream production.

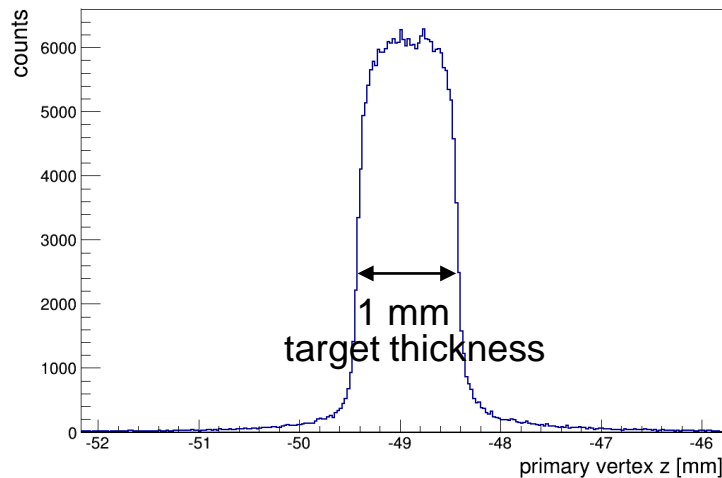


Angle distribution

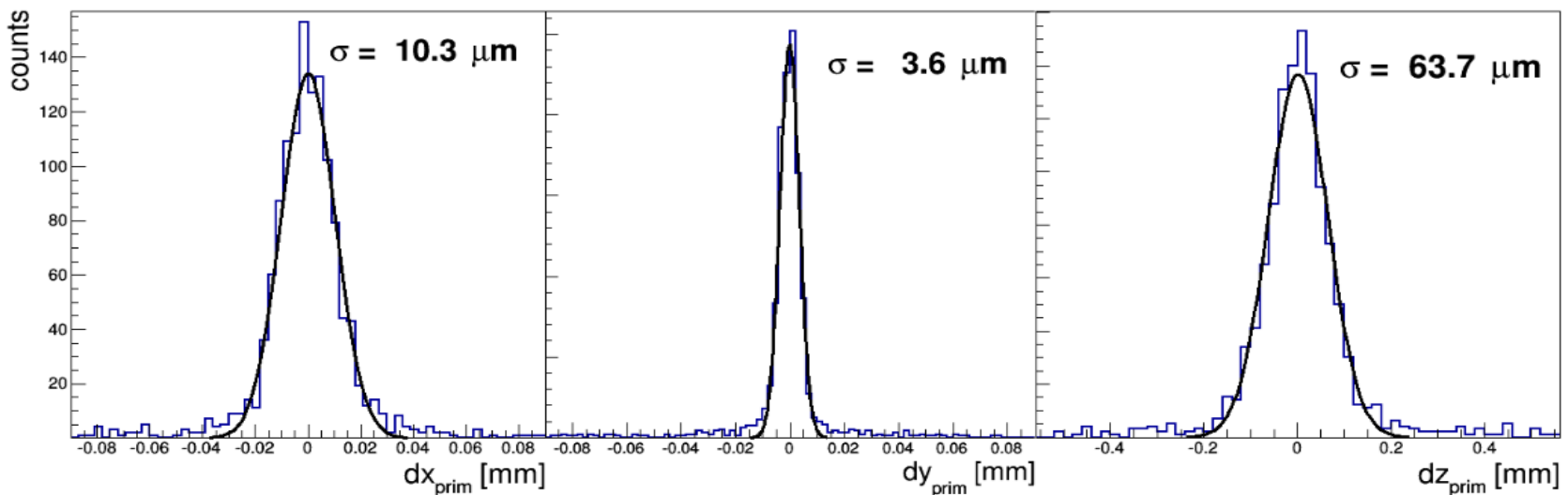
- Reconstruction of the primary vertex



Primary vertex reconstruction



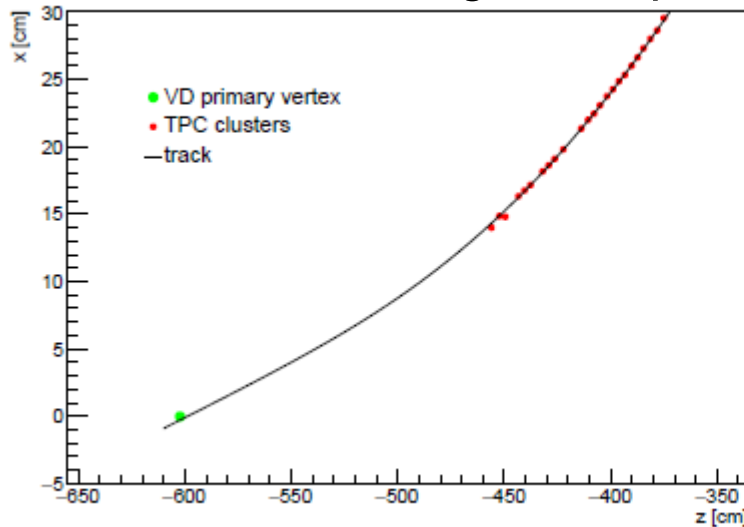
- Spatial resolution of the primary vertex: $\sigma_x = 5 \mu\text{m}$, $\sigma_y = 1.5 \mu\text{m}$ and $\sigma_z = 30 \mu\text{m}$.
- The difference between σ_x and σ_y can be attributed to the presence of the vertical component of the magnetic field which deteriorates description of tracks trajectories in the x direction.



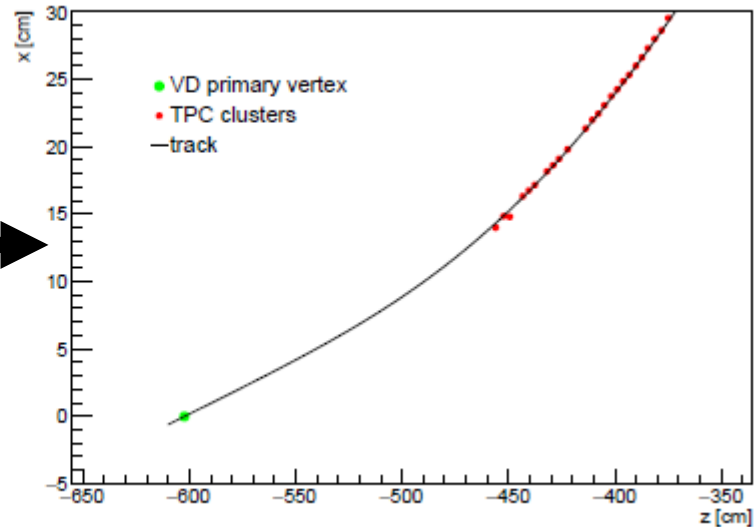
Matching algorithm

- Track matching between VD and TPC is done using the following algorithm: tracks are fitted to the VD primary vertex and then interpolated to other VD stations and the matching clusters are collected;
- Finally, the whole track is refitted using the Kalman Filter.

Before refitting to VD primary vertex

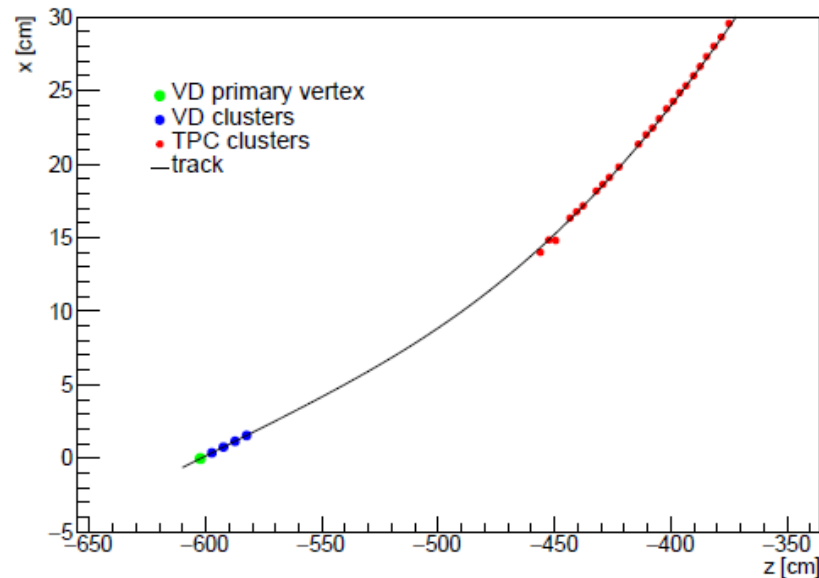


After



Matching algorithm

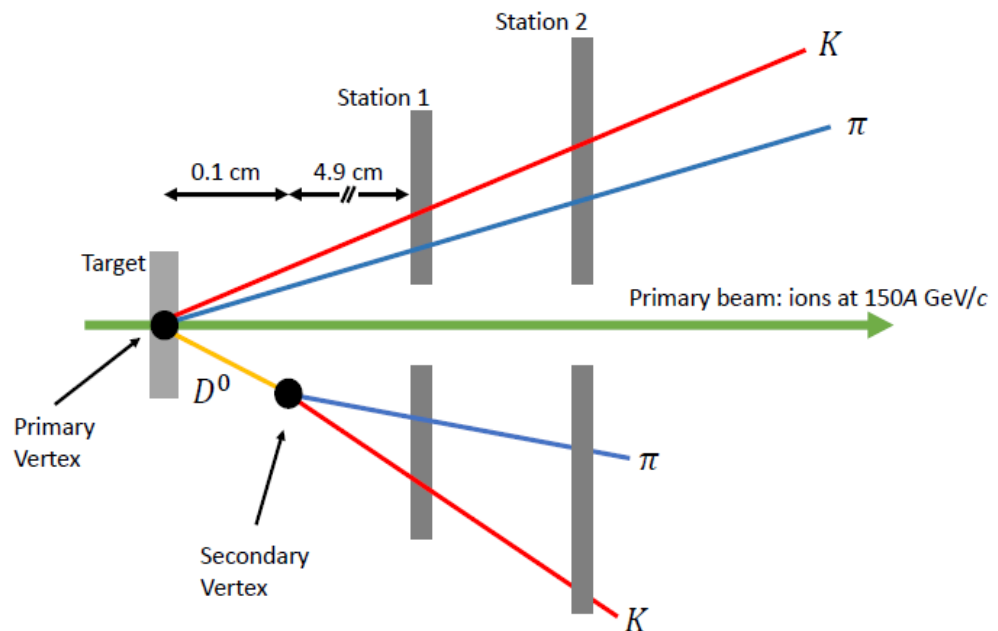
- Track matching between VD and TPC is done using the following algorithm: tracks are fitted to the VD primary vertex and then interpolated to other VD stations and the matching clusters are collected;
- Finally, the whole track is refitted using the Kalman Filter.



Reconstruction of D^0 signal

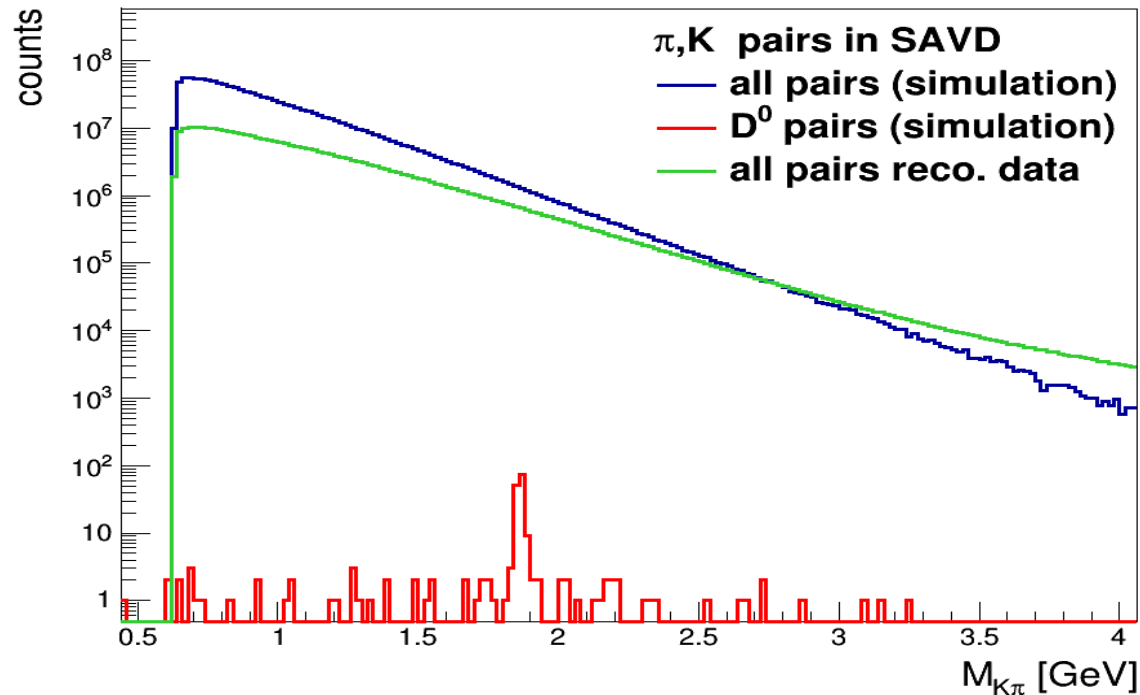
Meson	Decay channel	$c\tau$	Branching ratio
D^0	$D^0 \rightarrow K^- + \pi^+$	$122.9 \mu\text{m}$	$(3.91 \pm 0.05)\%$
D^0	$D^0 \rightarrow K^- + \pi^+ + \pi^+ + \pi^-$	$122.9 \mu\text{m}$	$(8.14 \pm 0.20)\%$
D^+	$D^+ \rightarrow K^- + \pi^+ + \pi^+$	$311.8 \mu\text{m}$	$(9.2 \pm 0.25)\%$
D_s^+	$D_s^+ \rightarrow K^+ + K^- \pi^+$	$149.9 \mu\text{m}$	$(5.50 \pm 0.28)\%$
D^{*+}	$D^{*+} \rightarrow D^0 + \pi^+$...	$(61.9 \pm 2.9)\%$

D^0 -meson can be reconstructed by its two body decay channel



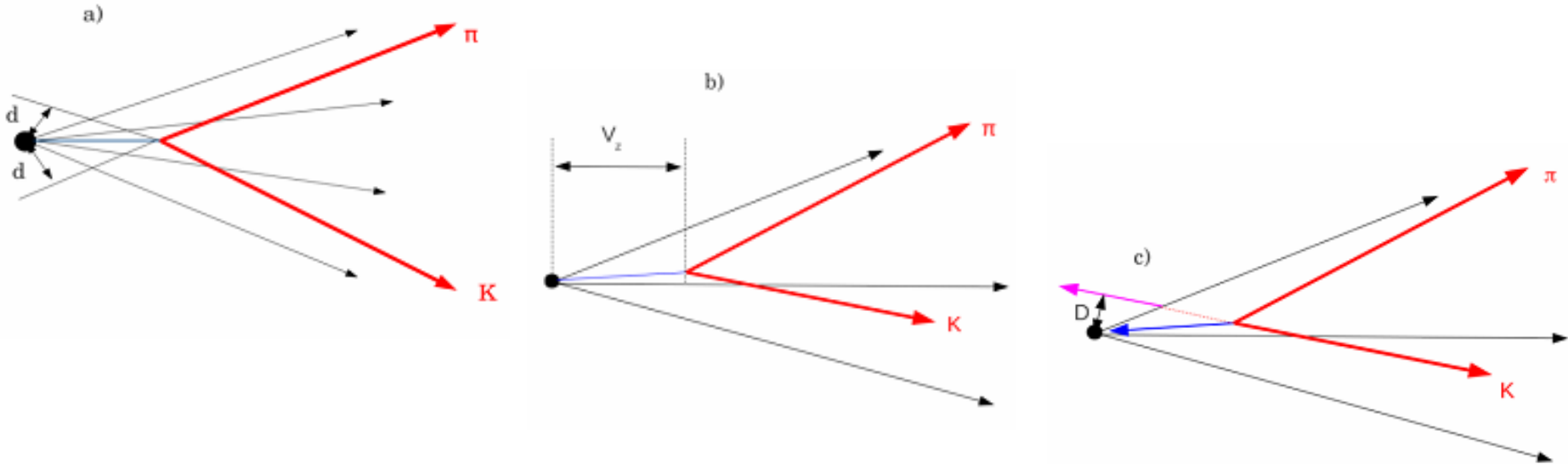
Reconstruction of D^0 signal

- SAVD tracks matched to TPC tracks are used in the search for the D^0 signal;
- Each SAVD track is paired with another SAVD track and is assumed to be either a kaon or pion;
- To suppress the background one needs to introduce cuts.



Open charm cuts

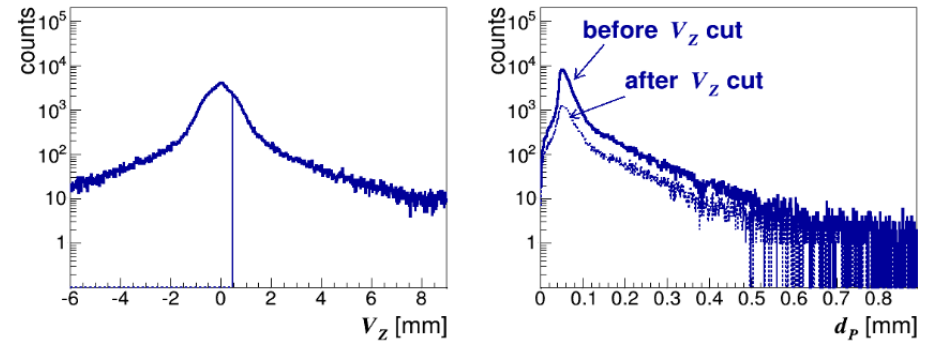
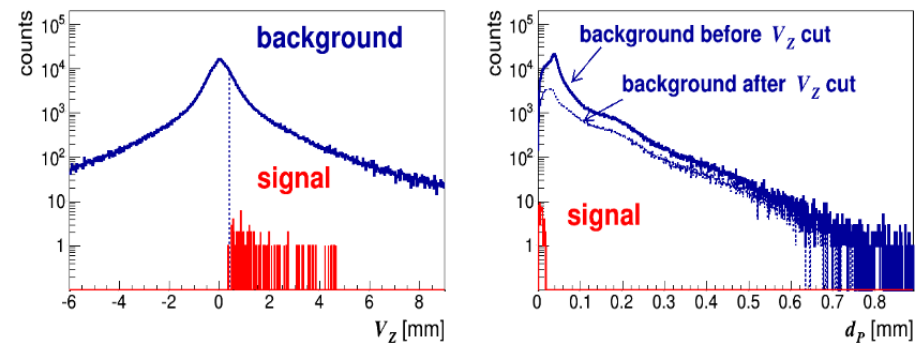
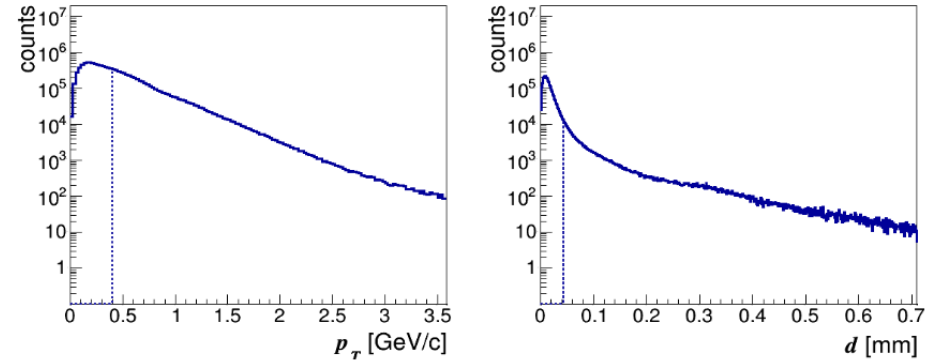
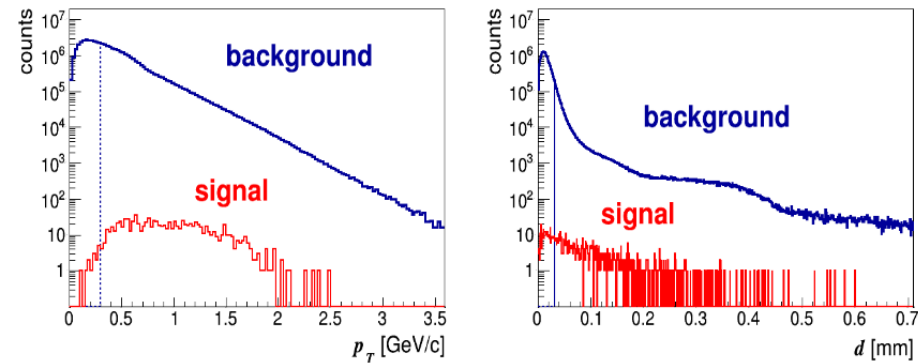
- Cut on **transverse momentum** $p_T > 0.31 \text{ GeV}/c$;
- (a) Cut on the track **impact parameter** $d > 31 \mu\text{m}$;
- (b) Cut on the **longitudinal position** $V_z > 400 \mu\text{m}$ of the track pair vertex relative to primary vertex;
- (c) Cut on the **parent particle impact parameter** $D < 20 \mu\text{m}$.



Open charm cuts

simulation

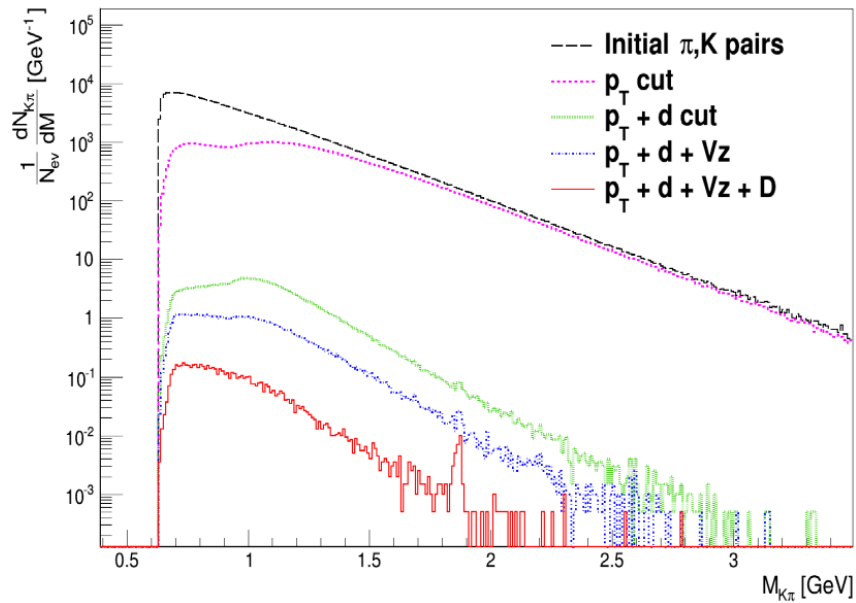
data



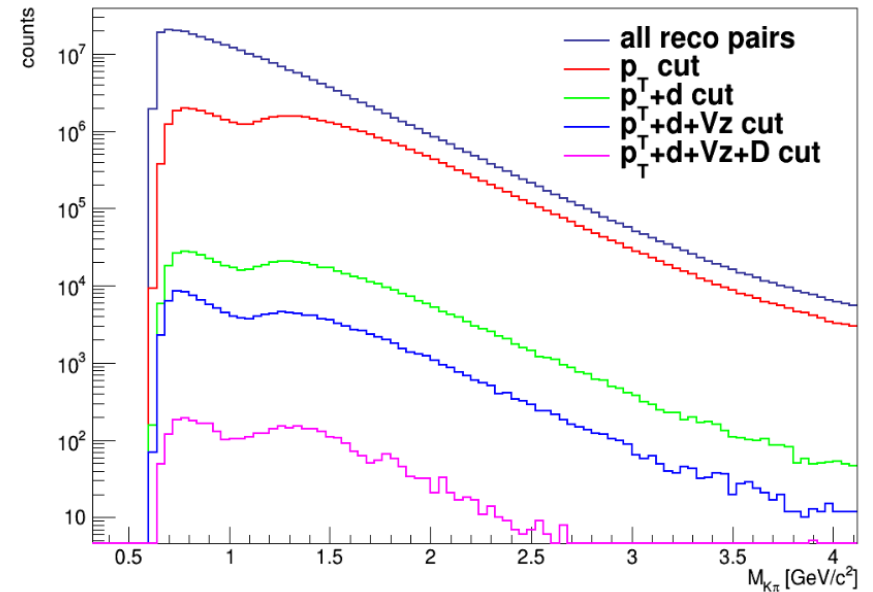
Data taking results

Open charm simulations

simulation

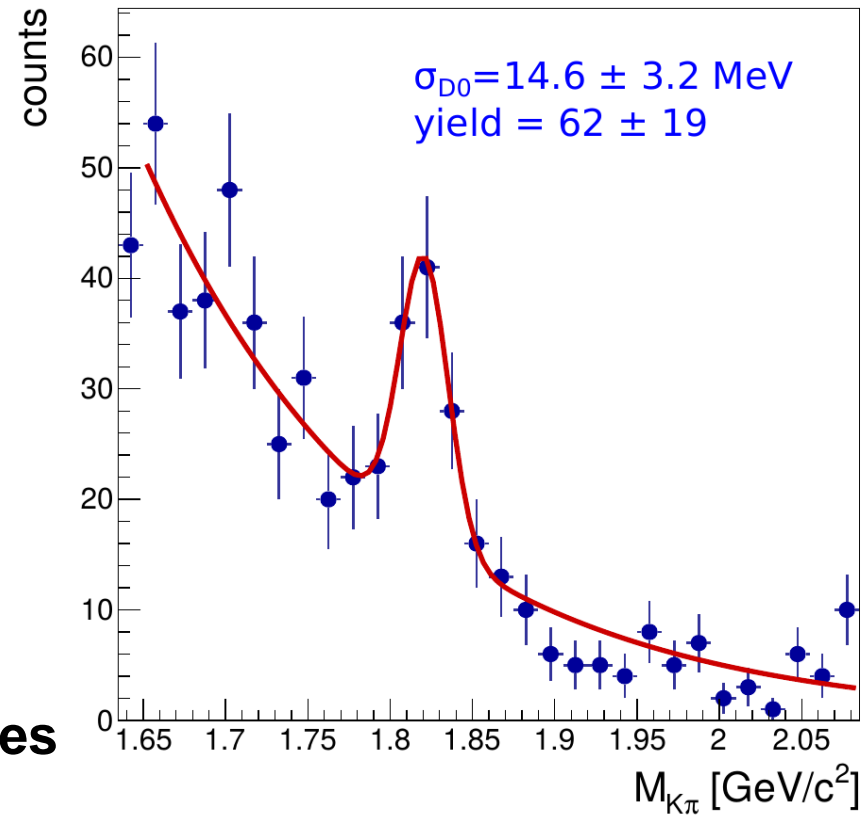


data



D⁰ & antiD⁰ signal reconstruction

- After reducing the background one may see a peak emerges at 1.8 GeV/c², which corresponds to D⁰ & antiD⁰ signal.

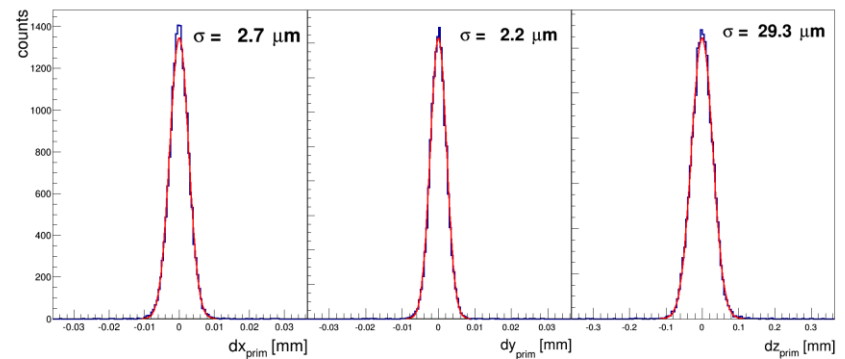
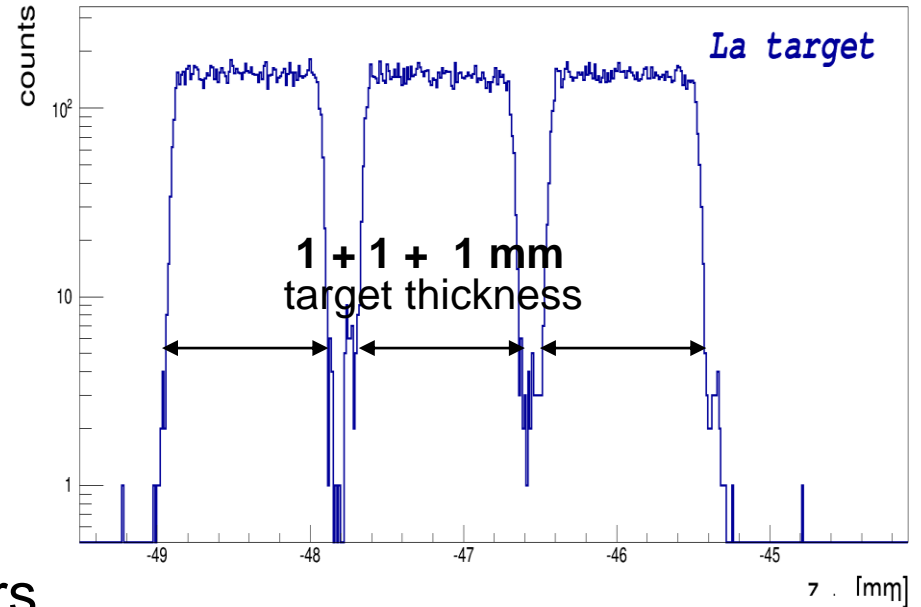


First observation of D⁰ peak in Pb+Pb collisions at SPS energies

Test data taking at 150A GeV/c

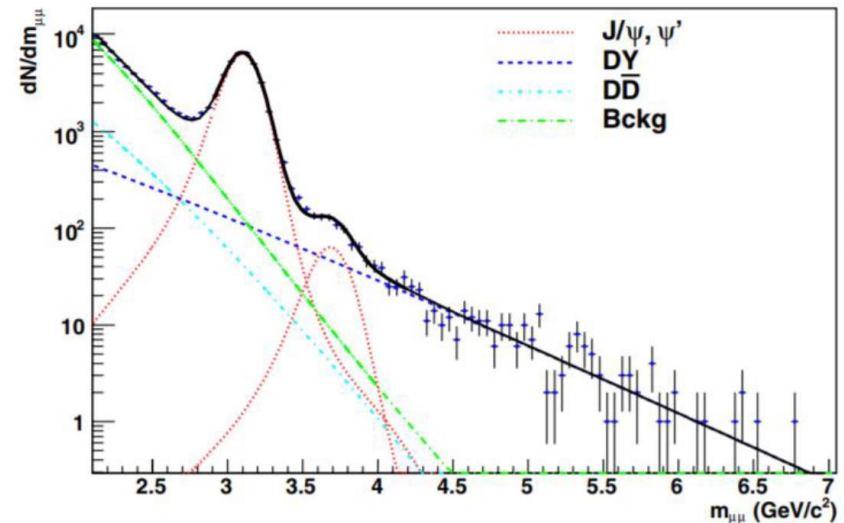
Xe+La data taking 2017

- XeLa 150GeV/c
 - target IN 4751k;
 - ~200k field off data;
- XeLa 75GeV/c
 - target IN 2551k;
- XeLa 40GeV/c
 - target IN 3748 k.
- La target consisted of 3 layers 1mm width.
- Spatial resolution of the primary vertex:
 $\sigma_x = 2.5 \mu\text{m}$, $\sigma_y = 1 \mu\text{m}$ and $\sigma_z = 15 \mu\text{m}$.



Importance of XeLa data

- J/ψ production in In+In ($A = 115$) collisions at 158A GeV/c was precisely measured by NA60.
- This data together with NA61 results on open charm production in Xe+La ($A = 129$, $A = 139$) collisions at 150A GeV/c will strongly challenge theoretical models.

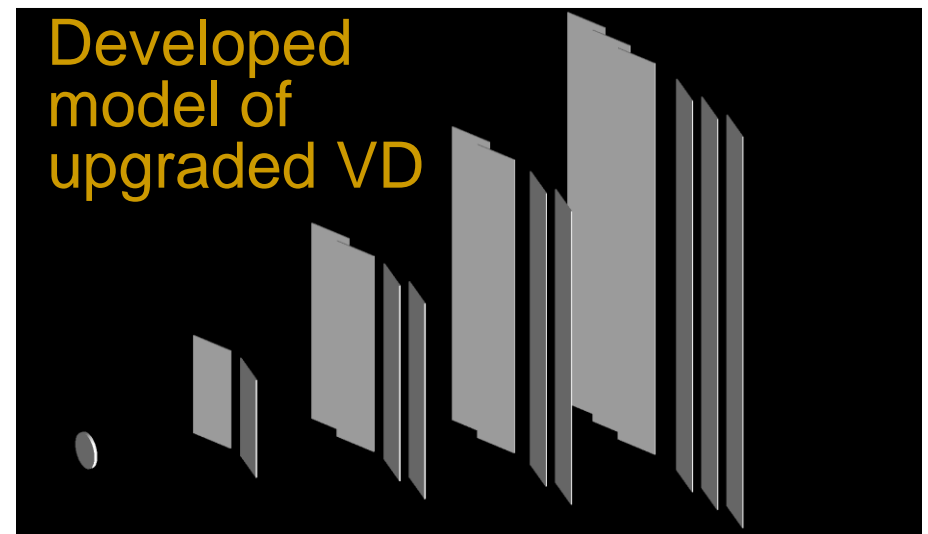
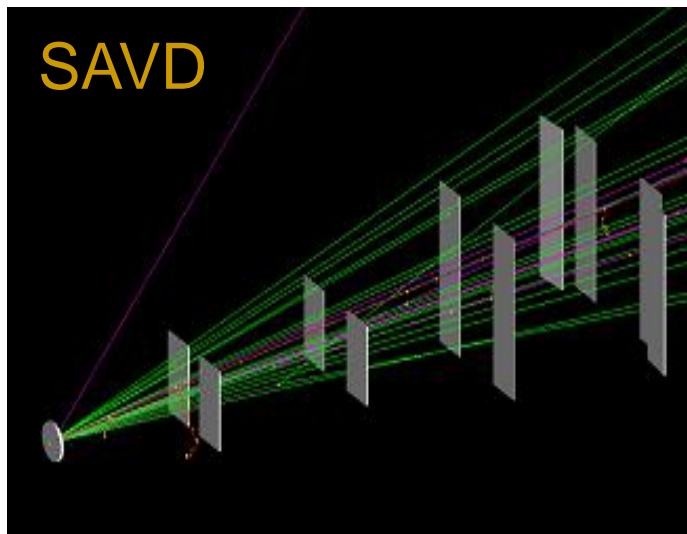


Summary & plans

- Data taking with Vertex Detector:
 - **2016 Dec**: Pb+Pb at 150A GeV/c
→ **first direct observation of D^0 signal in nucleus-nucleus collisions in fixed target experiment;**
 - **2017 Nov–Dec** : Xe + La run at 150A, 75A and 40A GeV/c
→ reconstruction is ongoing;
 - **2018 Nov-Dec**: Pb+Pb at 150A GeV/c
Open Charm production beam time;
Expected to collect 10M central events.

Upgraded Vertex Detector

- Looking forward, an upgraded version of SAVD so-called **Vertex Detector** (VD) with more sensors is being planned after upgrade of NA61 to 1kHz trigger rate after 2021.



Upgraded Vertex Detector

- The upgraded VD will be based on developed ALICE ITS technology: **ALPIDE** sensors, carbon fiber support structures and read-out electronics.
- Using of ALPIDE sensors will allow to reduce the read-out time to $10\mu\text{s}$;
- ALPIDE have very low noise level (more than 2 orders lower the MIMOSA-26);
- ALPIDE fulfills radiation hardness requirements.

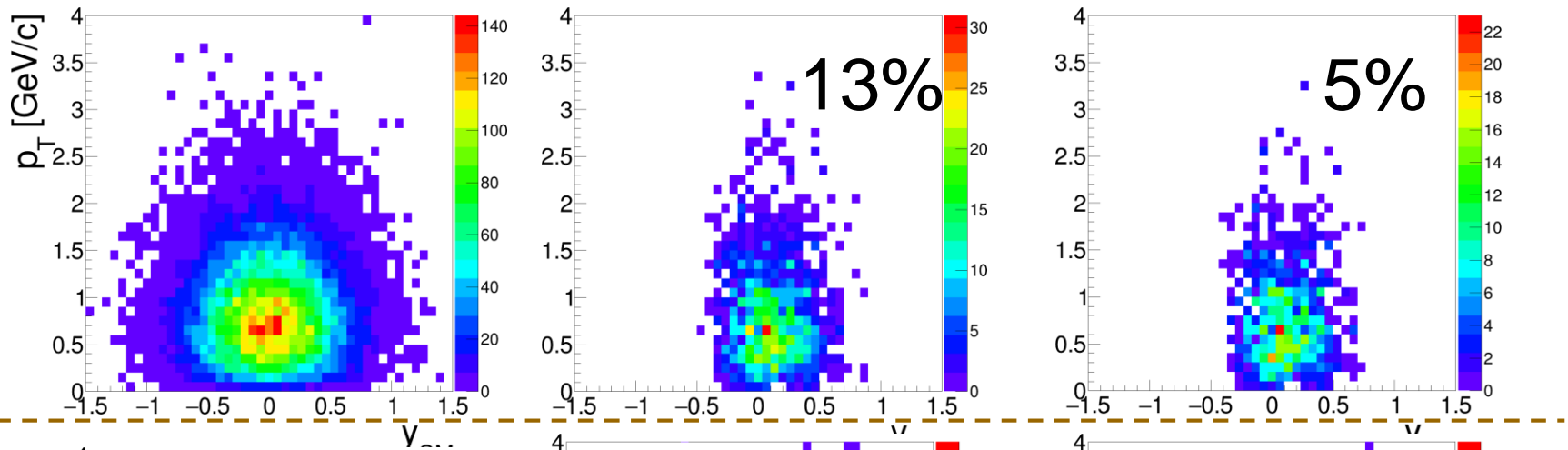


	MIMOSA-26AHR	ALPIDE
Sensor thickness (μm)	50	50
Spatial resolution (μm)	3.5	5
Dimensions (mm^2)	10.6×21.2	13.8×30
Power density (mW/cm^2)	40	40
Time resolution (μs)	115.2	10
Detection efficiency (%)	>99	>99
Dark hit occupancy	$\lesssim 10^{-4}$	$\lesssim 10^{-6}$

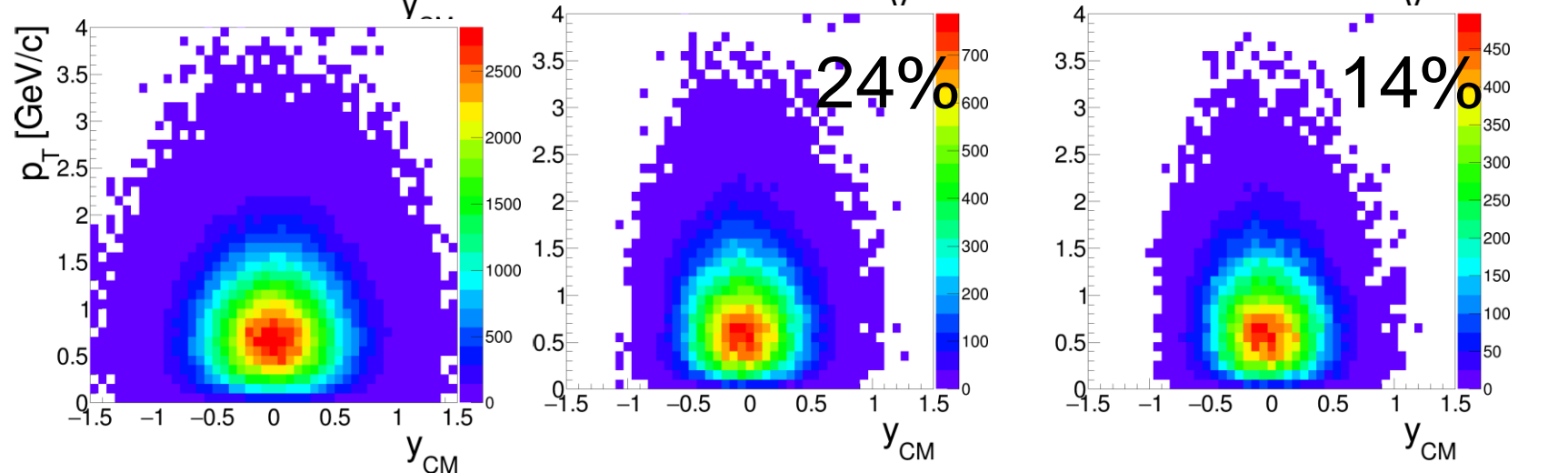
Upgraded VD vs SAVD

Increasing the VD acceptance: $32\text{cm}^2 \rightarrow 190\text{ cm}^2$

SAVD



upgraded VD



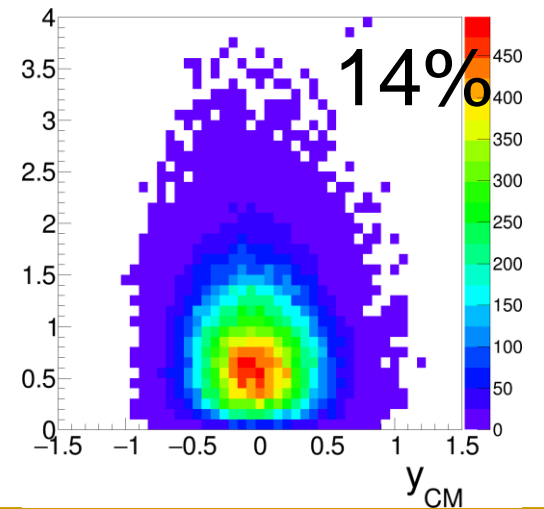
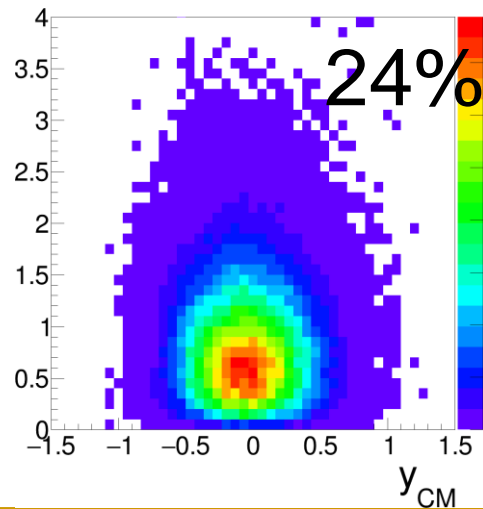
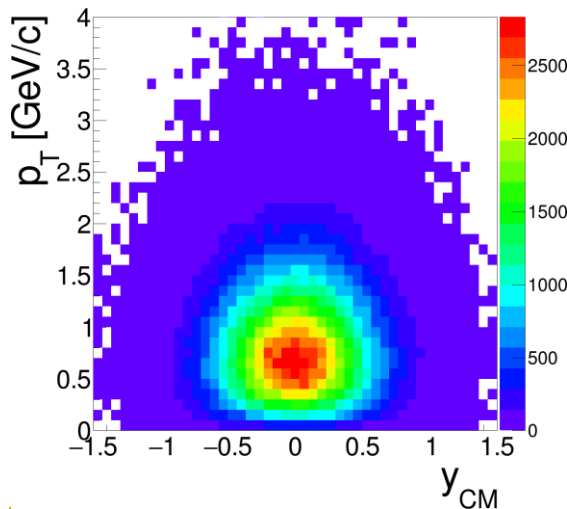
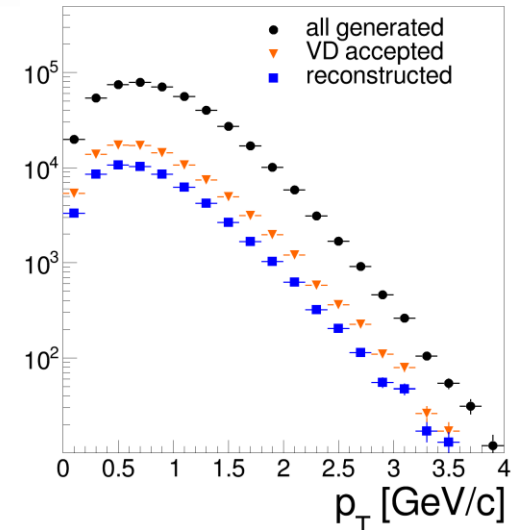
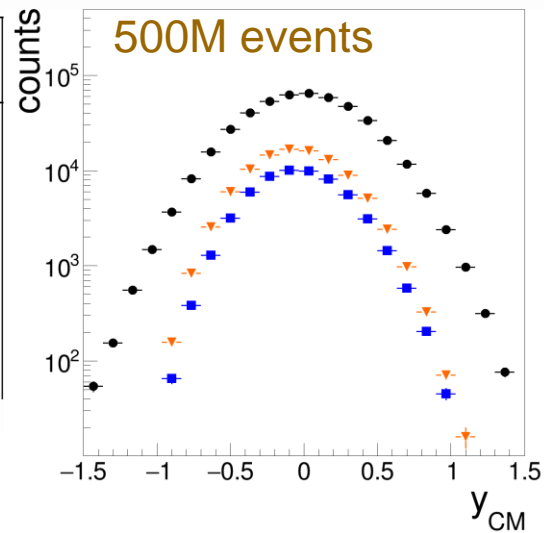
All generated

VD&TPC accepted

Accepted with cuts

Upgraded Vertex Detector: D0& antiD0

Meson	Decay channel
D^0	$D^0 \rightarrow K^- + \pi^+$
D^0	$D^0 \rightarrow K^- + \pi^+ + \pi^+ + \pi^-$
D^+	$D^+ \rightarrow K^- + \pi^+ + \pi^+$
D_s^+	$D_s^+ \rightarrow K^+ + K^- \pi^+$
D^{*+}	$D^{*+} \rightarrow D^0 + \pi^+$



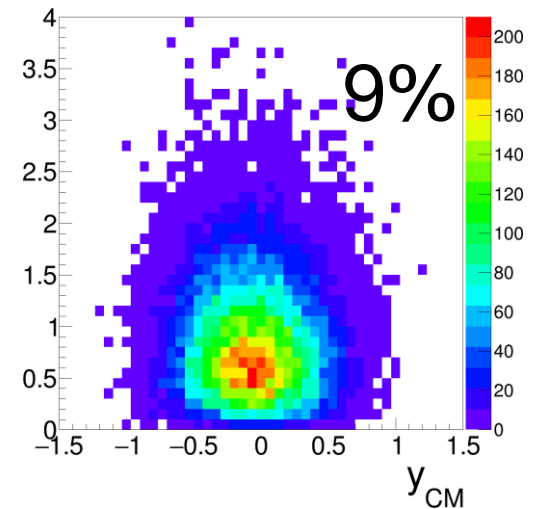
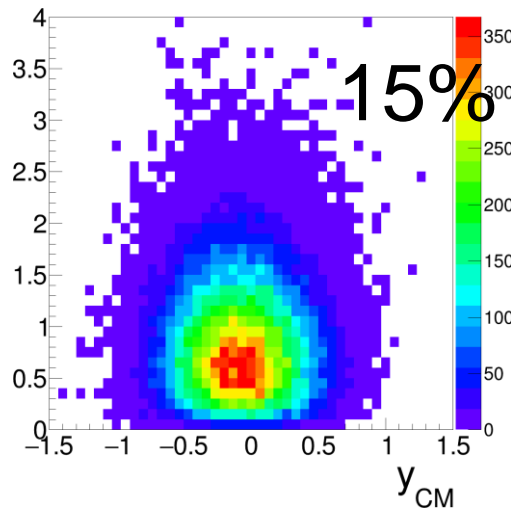
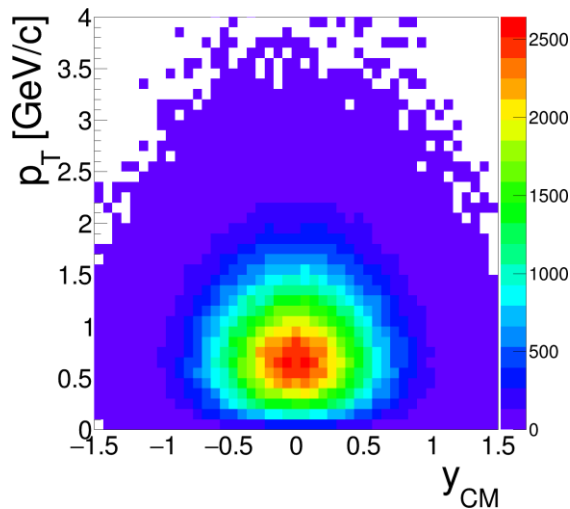
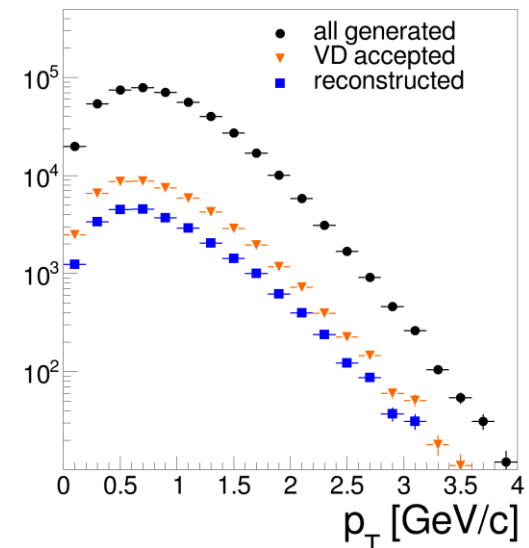
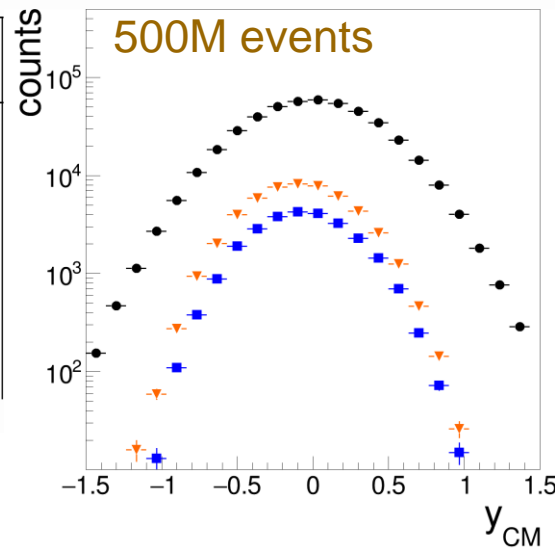
All generated

VD&TPC accepted

Accepted with cuts

Upgraded Vertex Detector: D+ & D-

Meson	Decay channel
D^0	$D^0 \rightarrow K^- + \pi^+$
D^0	$D^0 \rightarrow K^- + \pi^+ + \pi^+ + \pi^-$
D^+	$D^+ \rightarrow K^- + \pi^+ + \pi^+$
D_s^+	$D_s^+ \rightarrow K^+ + K^- + \pi^+$
D^{*+}	$D^{*+} \rightarrow D^0 + \pi^+$



All generated

VD&TPC accepted

Accepted with cuts

Expected open charm measurements

- Precise measurements of charm hadron production by NA61/SHINE are expected to be performed in 2021–2023.
- This would be first detailed study of open charm production in the SPS energy domain.

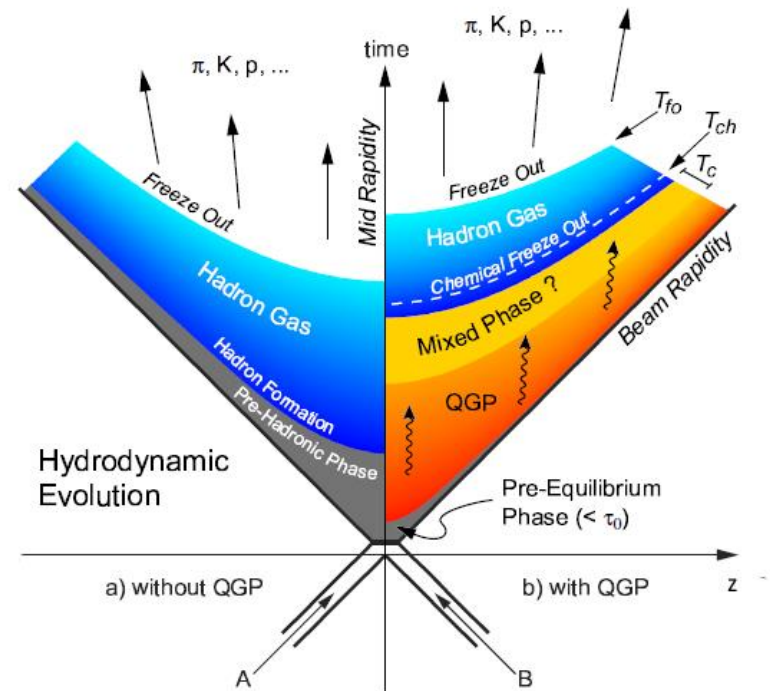
Year	Reaction	Number of events	D ⁰ & antiD ⁰	D ⁺ & D ⁻
2021	Pb+Pb 150A GeV/c	250M	38k	23k
2022	Pb+Pb 150A GeV/c	250M	38k	23k
2023	Pb+Pb 40A GeV/c	250M	3.6k	2.1k

- The measurements will provide the long-awaited data crucial for the following topics:
 - J/ψ production as the signal of deconfinement;
 - Open charm yield as signal of deconfinement;
 - Open charm production mechanism: pQCD vs Statistical models.

Thank you for your attention!

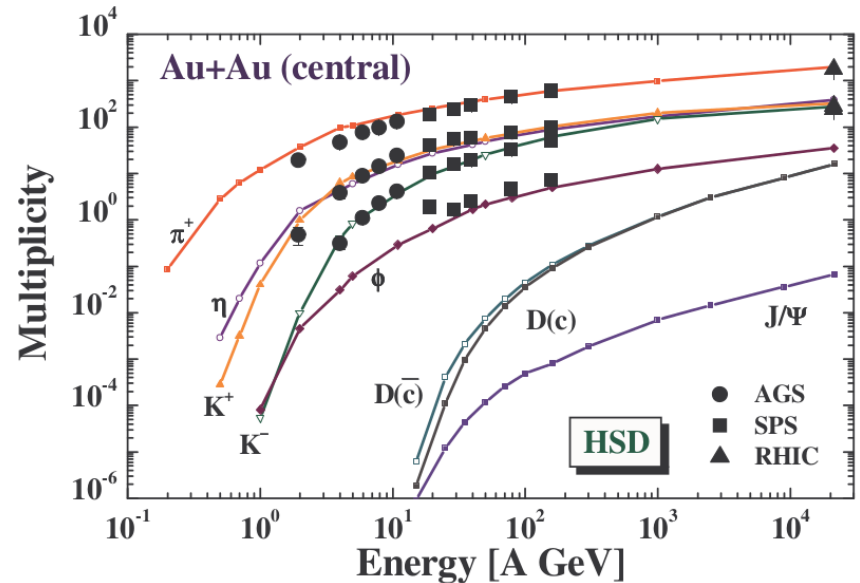
Quark-gluon plasma

- Quark-gluon plasma (QGP) is a state of matter in which partons (quarks and gluons) are **not confined in the hadrons**;
- The Big Bang theory predicts the formation of QGP at the very early stage of the Universe;
- The phase transition to QGP is expected to occur when the energy density of the system is high enough.
- Two possible scenarios of the space-time evolution of such a collision
 - In the first one (left) the energy density is not high enough to create quark-gluon plasma.
 - The second scenario (right) presents the collision with QGP formation.



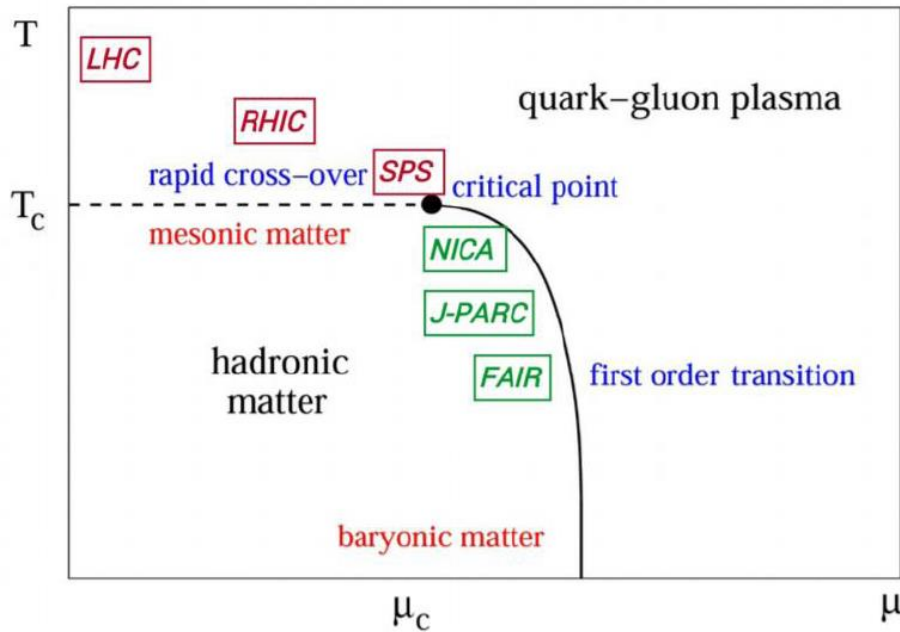
HSD

- Calculated meson multiplicities increase monotonically with the collision energy, which is in agreement with the data.
- The Hadron String Dynamics (HSD) predictions could be used for D and J/ψ production to estimate the required efficiency and beam intensity.
- Also according to these predictions, charm meson measurements are rather challenging because multiplicities are orders of magnitude than for other mesons.
- However, experimental studies of charm production could be performed not only for high energies, but also at lower energies such as 30A and 40A GeV/c.



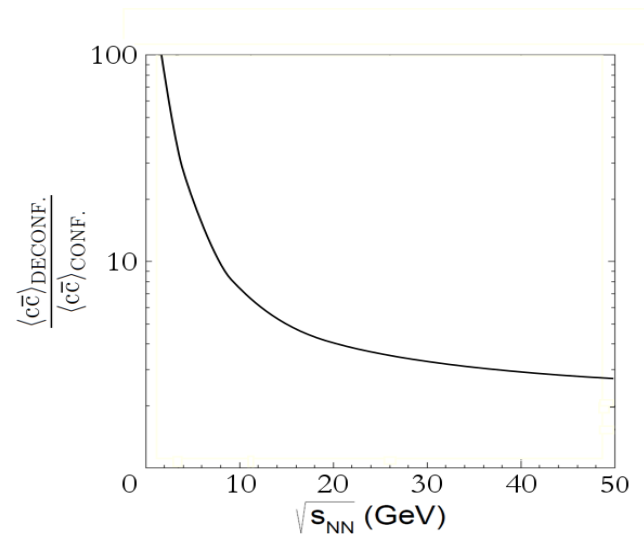
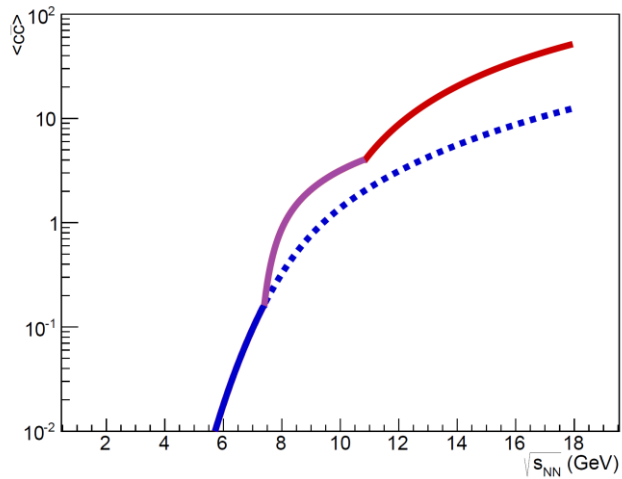
- Multiplicities of π , η , K^+ , K^- , D, D and J/ψ in the central Au+Au collisions from SIS to RHIC energies as predicted by HSD model and experimental data.

Uniqueness of NA61 open charm program



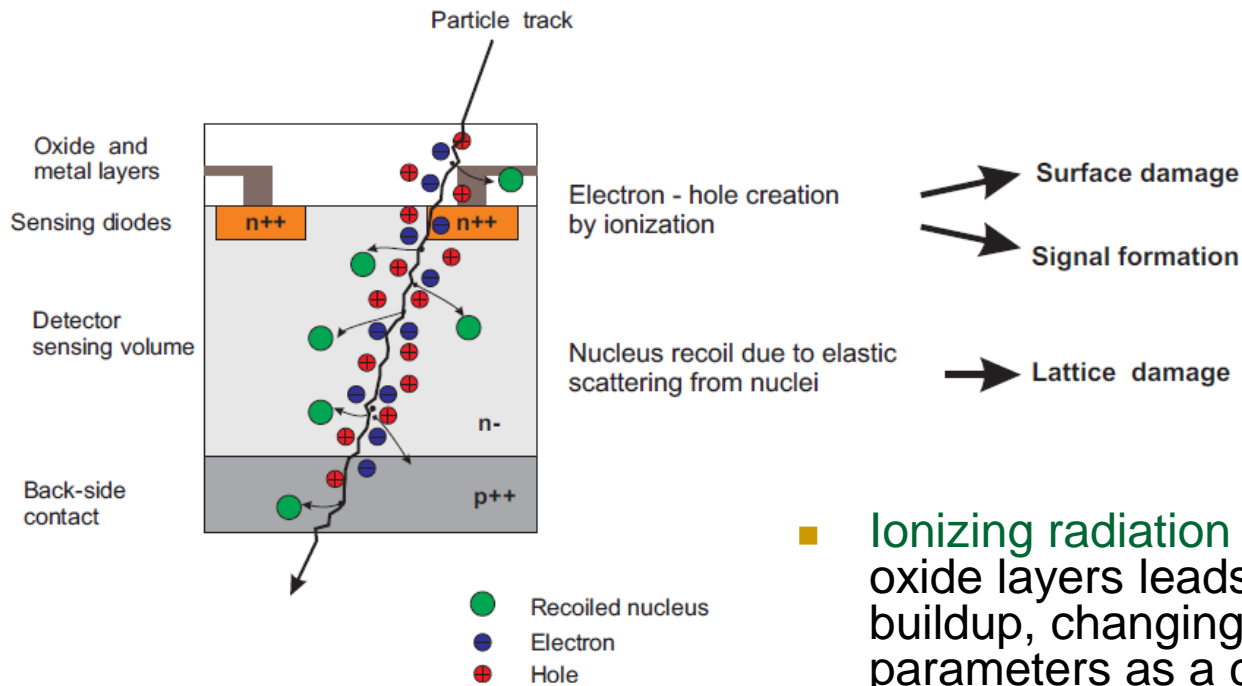
- **LHC and RHIC at high energies:** measurement in small phase space due to collider geometry and kinematics
- **RHIC BES collider:** measurement not possible due to collider geometry and kinematics
- **RHIC BES fixed-target:** measurement require dedicated setup – not under consideration
- **NICA (<80A GeV/c):** measurement during stage 2 under consideration
- **J-PARC (<20A GeV/c):** maybe possible after 2025
- **FAIR (<10A GeV/c):** not possible

Charm particles as a signal of deconfinement



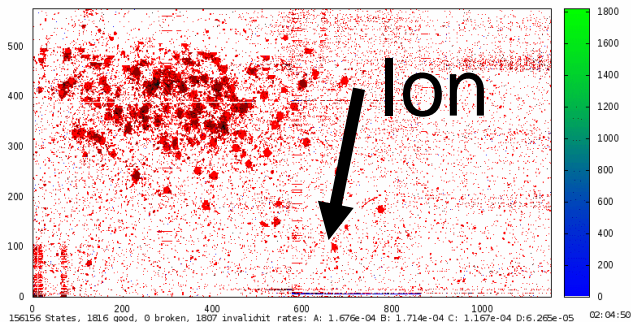
Open charm measurements motivation

Radiation damage

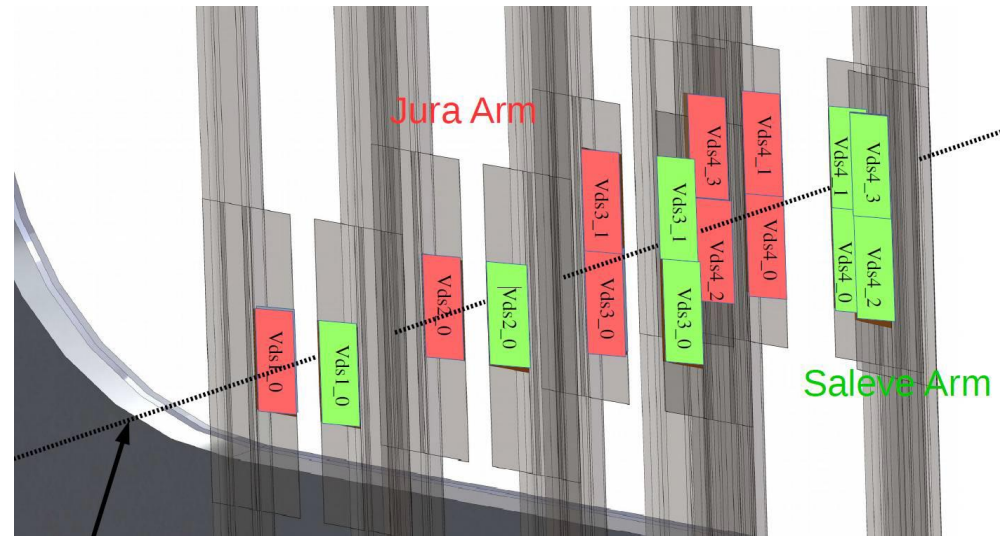


- **Ionizing radiation** passing through the oxide layers leads to a positive charge buildup, changing the electronic device parameters as a consequence.

- **The non-ionizing radiation** passing through the sensor displaces atoms from their positions in a lattice.
→ especially destructive for sensitive volume and leads to charge signal losses.



Sensor efficiencies



Station	Jura 2016	Jura 2017
1 - 0	72%	99%
2 - 0	94%	99%
3 - 0	61%	97%
3 - 1	31%	90%
4 - 0	50%	89%
4 - 1	62%	92%
4 - 2	41%	96%
4 - 3	0%	94%

Station	Saleve 2016	Saleve 2017
1 - 0	81%	85%
2 - 0	68%	99%
3 - 0	72%	92%
3 - 1	0%	85%
4 - 0	66%	97%
4 - 1	67%	97%
4 - 2	31%	96%
4 - 3	12%	93%

Radiation hardness

Radiation source	Ionizing	Non-ionizing
	[krad]	[$10^{12} n_{eq}/cm^2$]
Direct particles	35	1.3
Delta electrons	40	Negligible
Beam halo (scaled)	1200	2.0
Beam halo (measured)	200	0.3
Sum requirements	275-1275	3.3
ALPIDE	> 500	17.0

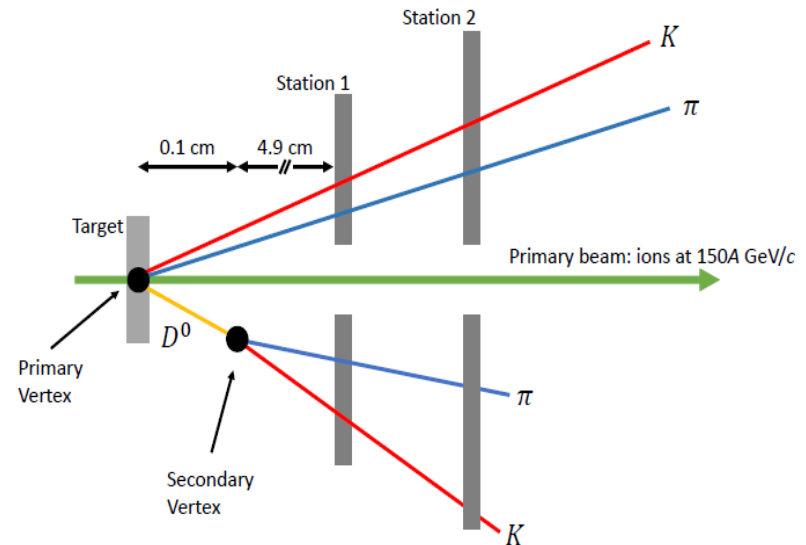
- VD to operate at a true collision rate of 5 kHz, and at a duty cycle of 0.15.
- Radiation doses at the most exposed point of the VD within a run of 40 days for the most exposed point of the VD;
- The radiation load dominated by the damage caused by direct beam ions from the beam halo, which varies substantially depending on the quality of the beam tuning.

Requirements for detector

- Rare probes of charm particles;
- Small distance between the decay vertices and the primary vertex.

→ general requirements for detector:

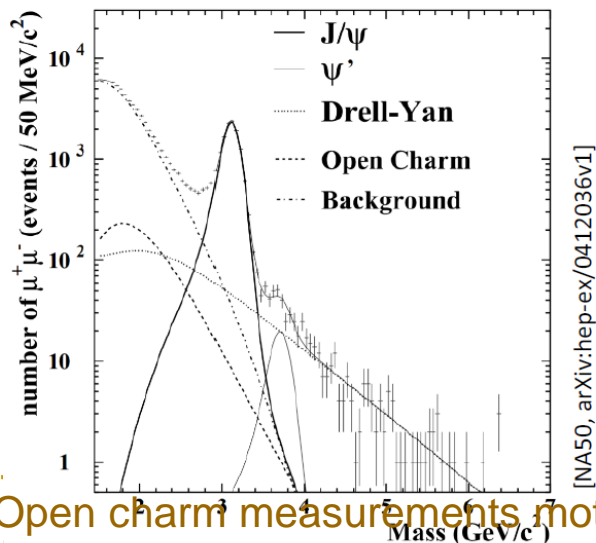
- Precise vertexing and tracking accuracy;
- High time resolution detectors;
- The lowest possible material budget in the tracking region in order to increase the efficiency of open charm measurements;
- High granularity of vertex tracking detectors capable to register the multiple tracks in A-A collisions.



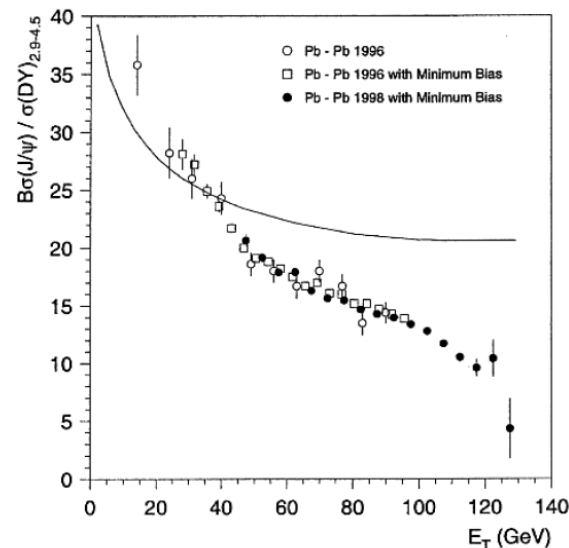
→ Vertex Detector project based on CMOS pixel detectors.

J/ψ production at CERN SPS

- The NA50 experiment that was interpreted as evidence for QGP creation in central Pb+Pb collisions at 158A GeV based on this assumption. However, the assumption $\langle cc_{\text{bar}} \rangle \sim \langle DY \rangle$ may be incorrect due to many effects, such as shadowing or parton energy loss;
- Up to now, only indirect measurements of open charm production in nucleus-nucleus collisions at the SPS energies exist and they are not reliable enough to distinguish the pQCD and statistical approaches to open charm production
 → One need direct **measurements of open charm yields.**



Open charm measurements motivation



The curve represents the J/ψ suppression due to ordinary nuclear absorption

Event reconstruction

- The event reconstruction is a challenging task due to the high charged particle multiplicities encountered in fixed target heavy ion collisions.

This task includes:

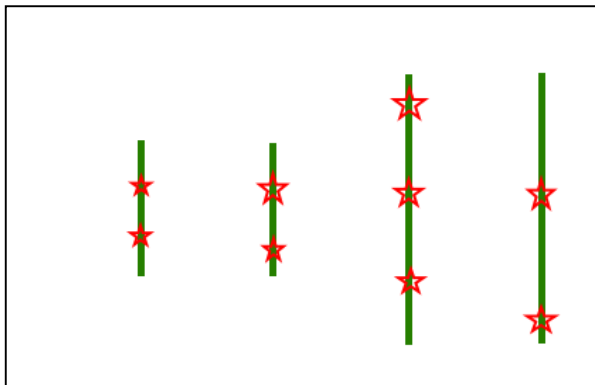
- Cluster reconstruction;
- Track reconstruction:
 - Track finding;
 - Track fitting;
- Primary vertex reconstruction;
- Secondary vertices reconstruction;
- Matching and refitting global tracks;
- Extracting physics.

Track reconstruction

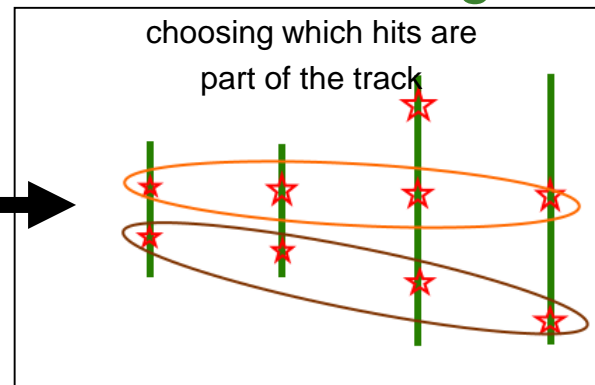
This task of track reconstruction is often divided into two different subtasks:

- **Track finding** (pattern recognition):
 - starts out with a set of position measurements (provided by a tracking detector). The aim is to group these measurements together in subsets, where each subset containing measurements from one traveling charged particle.
- **Track fitting** (parameter estimation):
 - for each of the subsets provided by the track finder, finds the optimal estimate of a set of parameters uniquely describing the state of the particle.

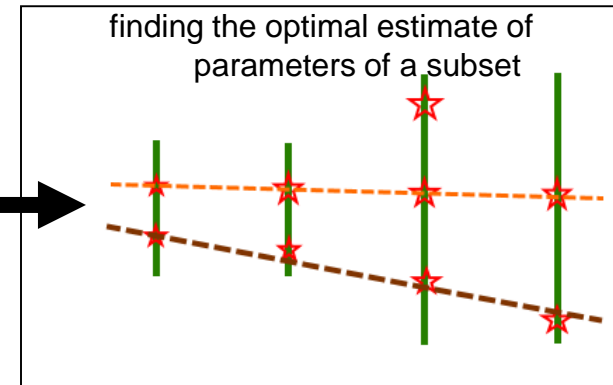
Measurements



Track finding



Track fitting



Track reconstruction in Vertex Detector

Track finding algorithms

1. Combinatorial method:

All possible combinations of the points are generated and checked against a track model. If the fit is good, the track candidate is accepted.

2. Local methods: (Ex: the Cellular Automaton)

Processes of track-finding are independent from each other.

- Some few points generate an initial track candidate;
- Using interpolation or extrapolation additional points are collected;
- When more points can be found the track candidate is assumed to be good, otherwise the track candidate is discarded;
- But local methods always contain unsuccessful track candidates.

3. Global methods: (Ex: the Hough Transform)

All points are processed by the algorithm in the same way.

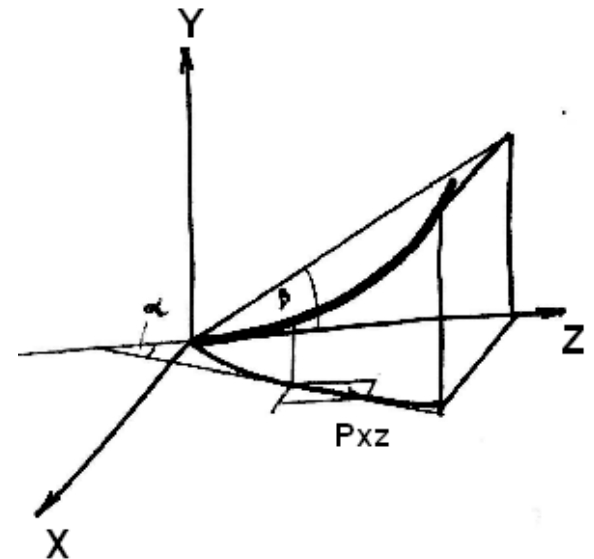
- Treats all hits in same manner, usually through some transformation;
- Every hit only processed once, the processing complexity of a global method in principle is proportional to the number of points within an event.

Hough Transform in magnetic field

- Track reconstruction is based on the **Hough transform**.
- It is a **global** method. It uses a parametric description of a track by a set of parameters.
- The magnetic field in Vertex detector volume is inhomogeneous (0.13÷0.25T).
- For particles with different momentum shapes of a curve differ;
- But on bright side curved tracks may allow for **momentum measurements**.
- Track model is chosen as **parabola** in (XZ) and **linear** in (YZ).

$$x = \frac{Ze}{|p|} B_y \frac{z^2}{2} + a_x z + b_x$$

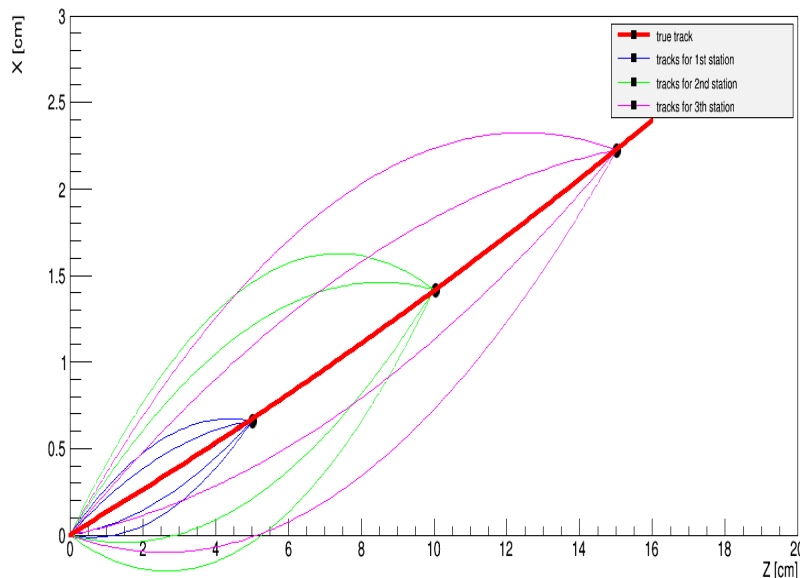
$$y = a_y z + b_y$$



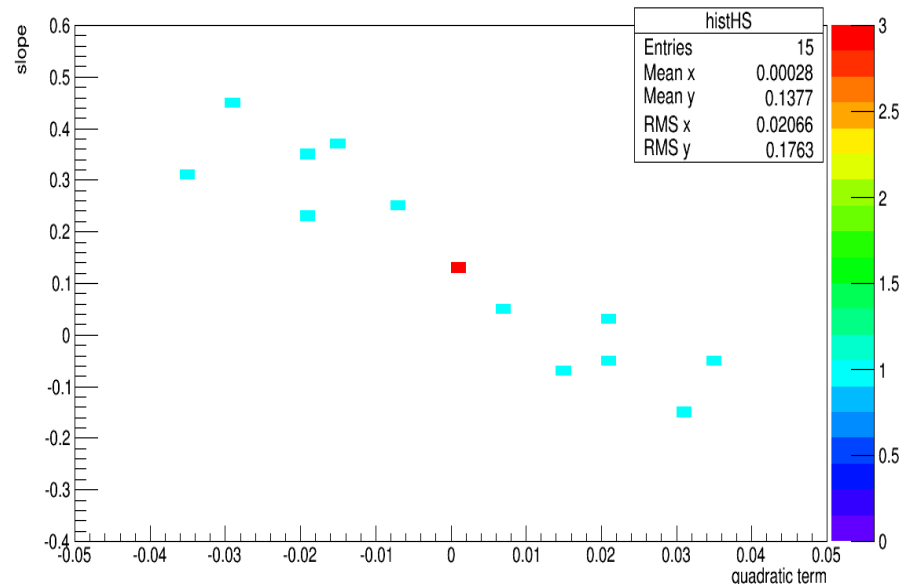
The algorithm of the Hough Transform

- ❑ Choosing parameterization for track;
- ❑ Converting the coordinates of the detector hits of particle tracks into the Hough space (space of track parameters);
- ❑ Accumulating sets of bins in histogram for each of the measurements in segment;
- ❑ Measurements that are lying along one track show up as peak in histogram. The voting procedure: object candidates are obtained as local maxima, so peaks assumed to correspond “real” tracks.

Image (XZ) Space

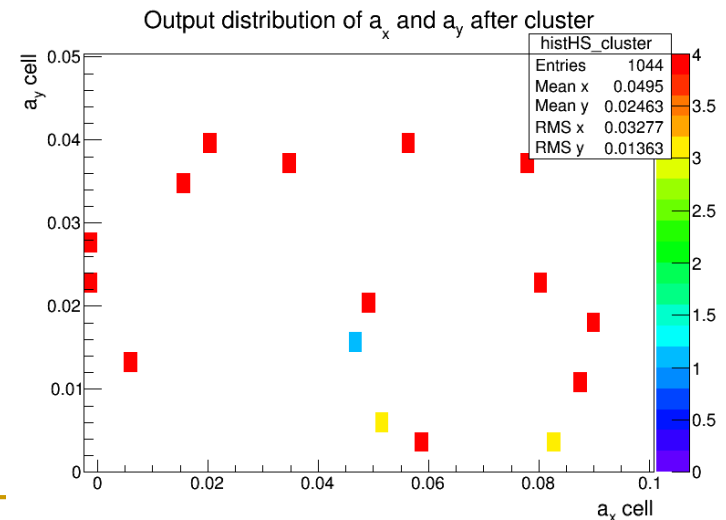
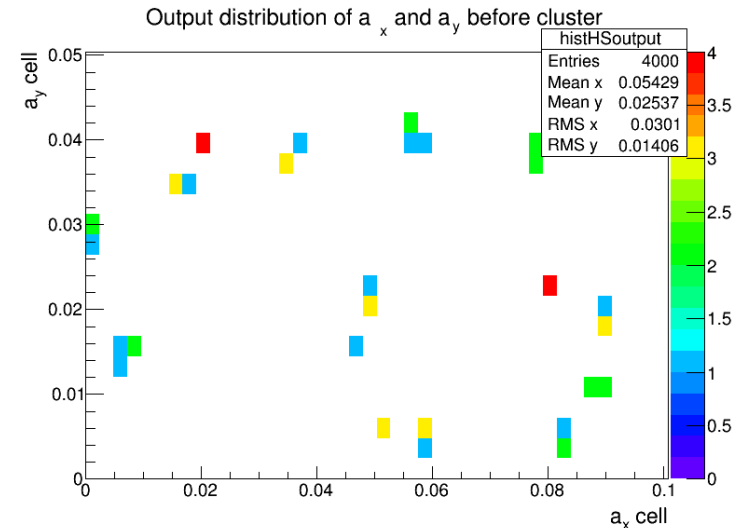


Hough Space



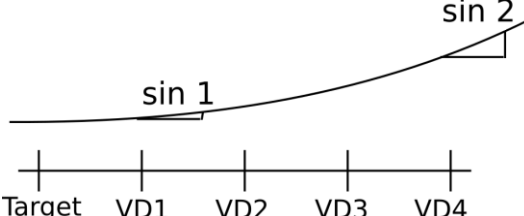
Implementation of the Hough Transform for the Vertex Detector

- Sometimes hits that belong to one track ends up in neighboring cells in Hough-space;
- The size (width) of the cells in the Hough Space have been determined according to uncertainty from multiple scattering, that depends on particle momentum;
- “Perfect” cell size does not exist;
- The problem of discretization of the accumulation Hough Space can be partly solved by clusterization, i.e. scanning Hough-space for neighboring cells and connecting counts in the accumulation space into clusters.



Momentum reconstruction

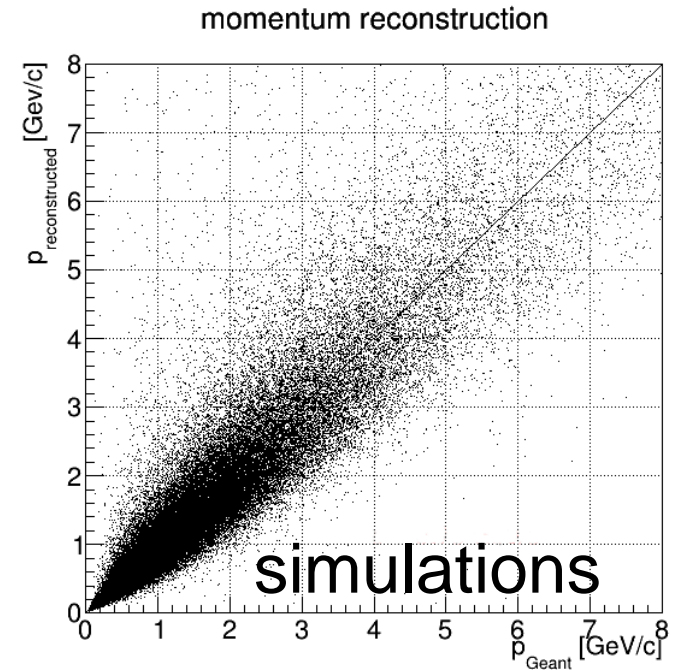
- Presence of the magnetic field in the volume of the Vertex Detector allows **momentum measurements**;
- Track momentum reconstruction method:
to integrate magnetic field over track length from VD1 to VD4.

$$p_{xz} = \frac{q \int B_y dl}{\sin 1 - \sin 2}$$


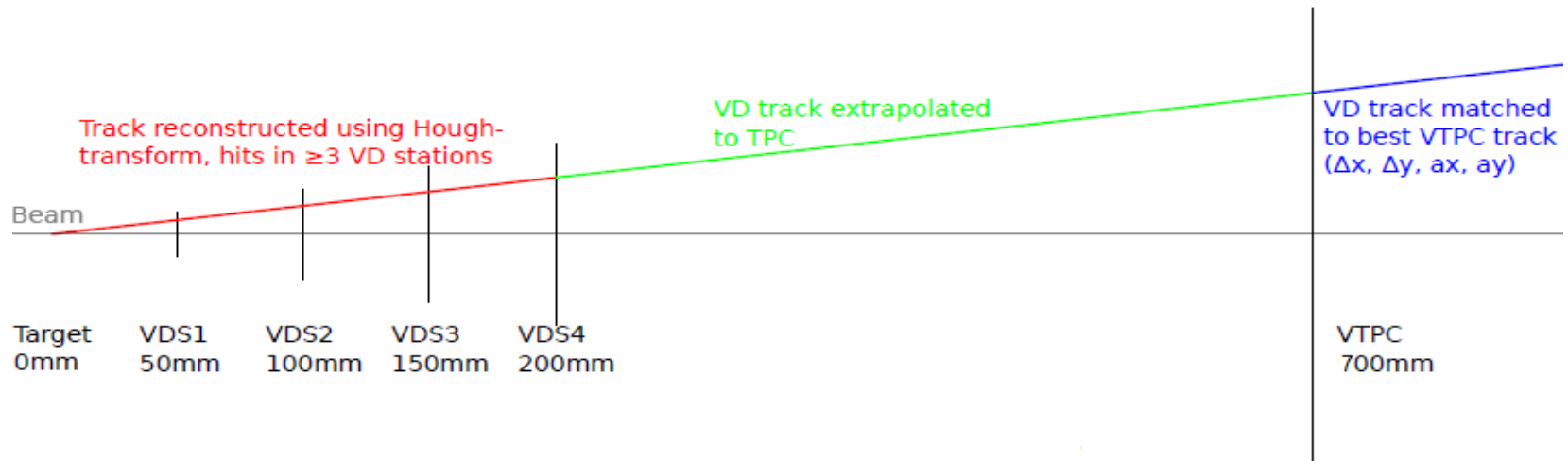
- Momentum resolution in stand-alone SAVD:

$$\frac{dp}{p} \sim 10^{-1}$$

- Momentum of VD tracks is not used directly
– this information we use to verify track matching procedure.

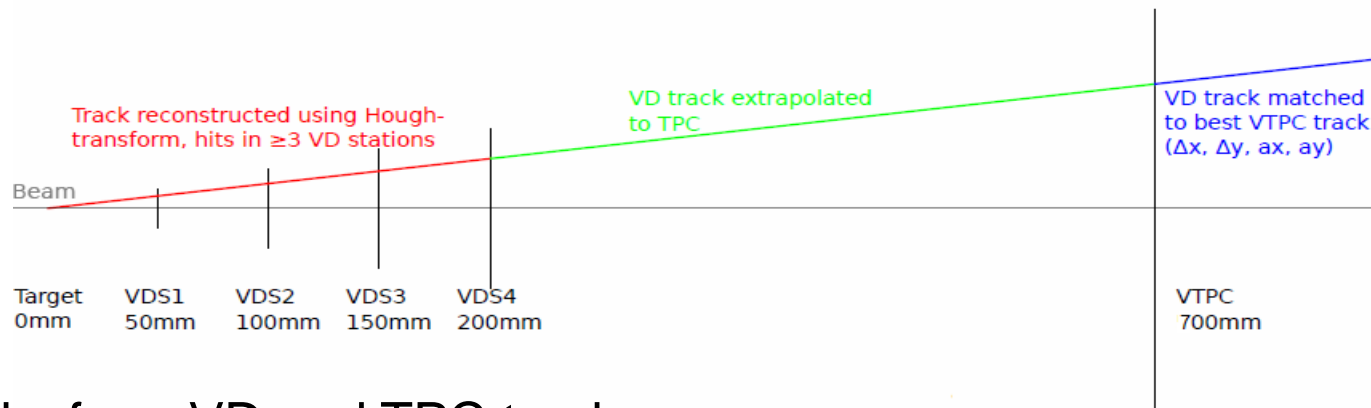


Matching algorithm

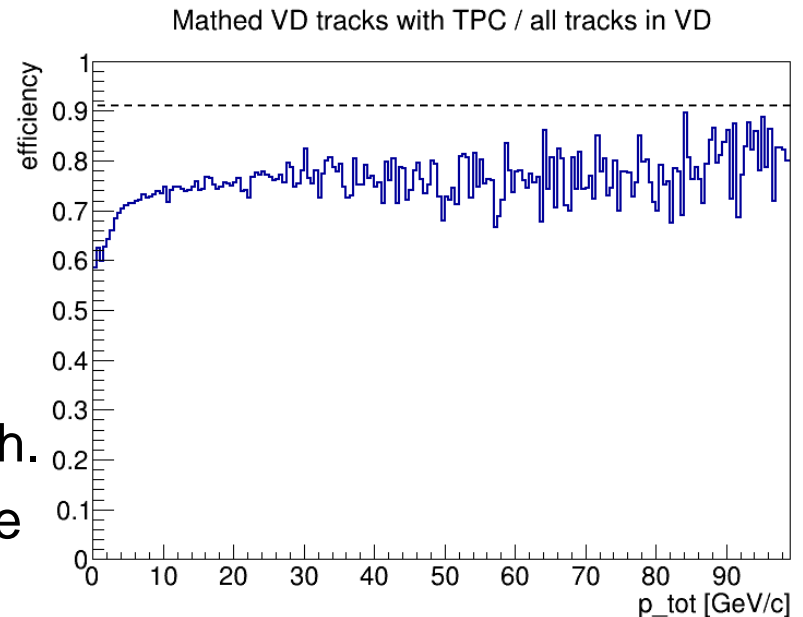


- Tracks from VD and TPC tracks are extrapolated to common plane (VTPC-1 surface);
- Find the best match over all combinations of VD and TPC tracks using basing of difference in the position and direction, and using charge and momentum to verify match.

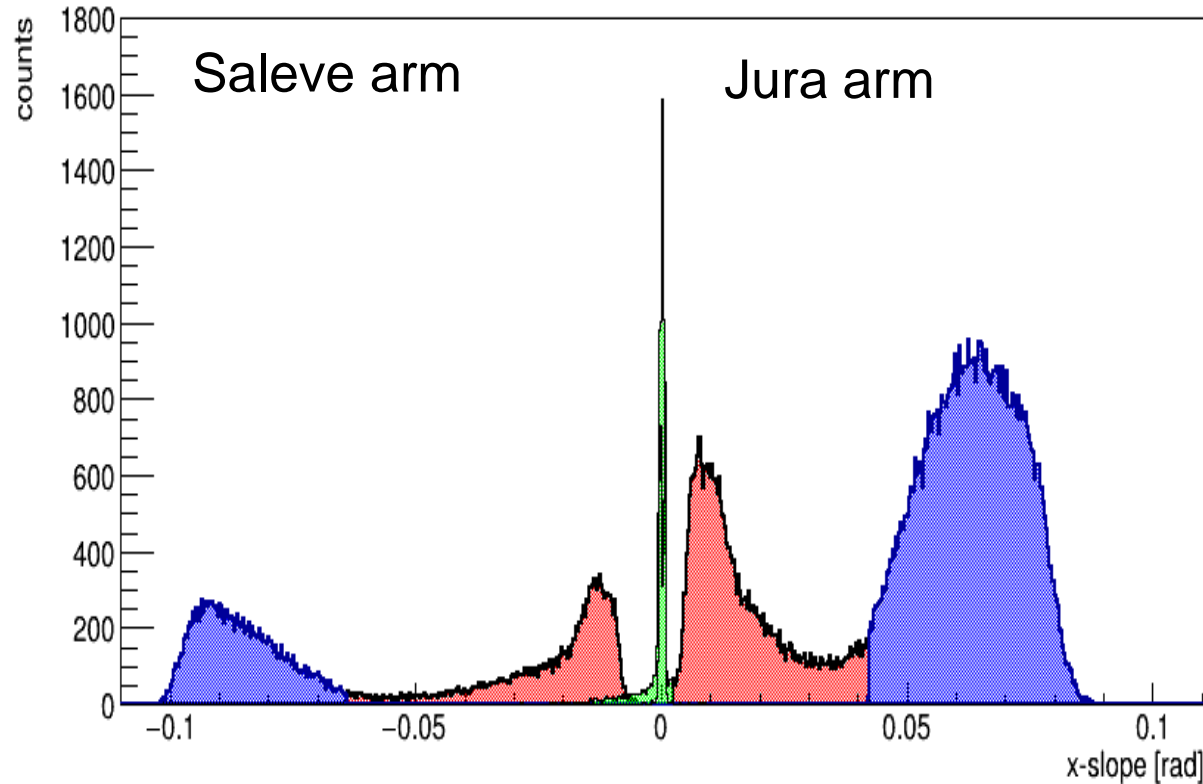
Matching algorithm



- Tracks from VD and TPC tracks are extrapolated to common plane (VTPC-1 surface);
- Find the best match over all combinations of VD and TPC tracks using basing of difference in the position and direction, and using charge and momentum to verify match.
- The track matching efficiency is on the level of 85%.

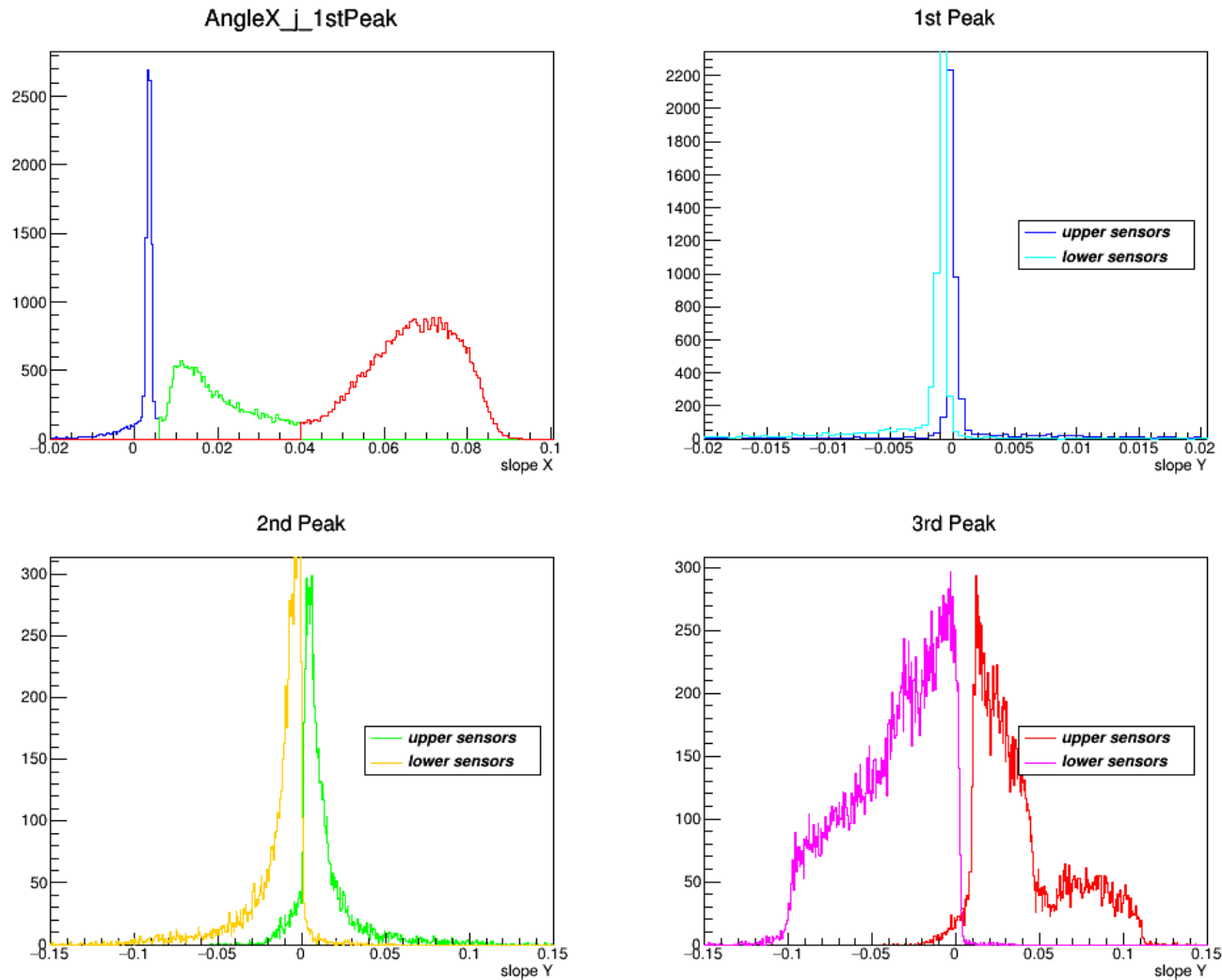


Angle distribution of the tracks

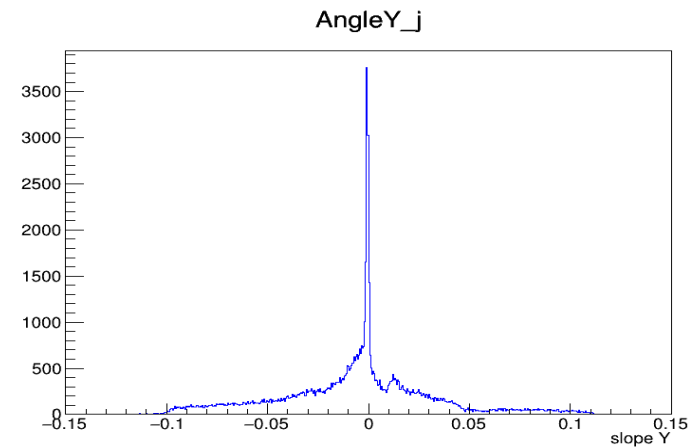
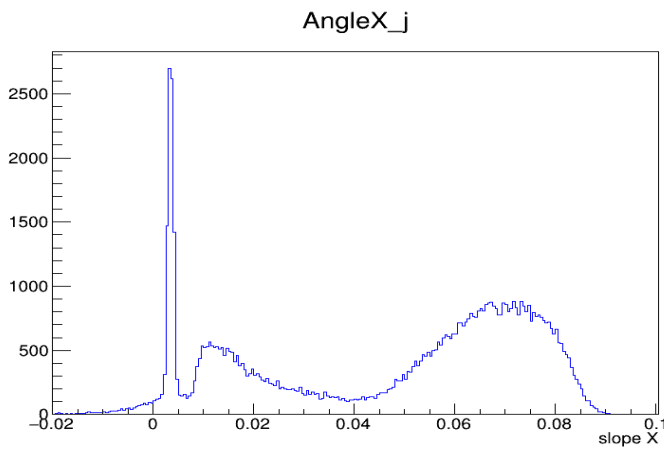


The angular distribution in x directions of the reconstructed tracks for Jura and Saleve arms has clear three peak structure.

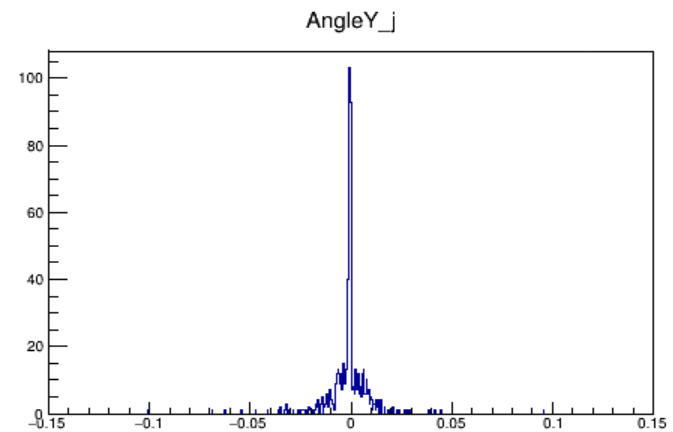
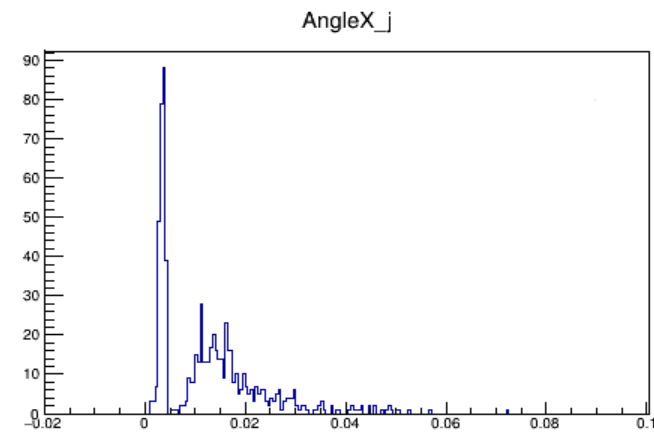
Angle distribution of tracks



Target IN and OUT angle distribution



Target IN



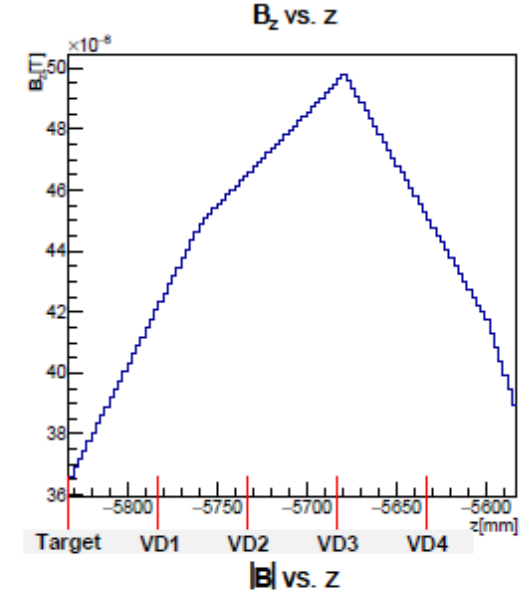
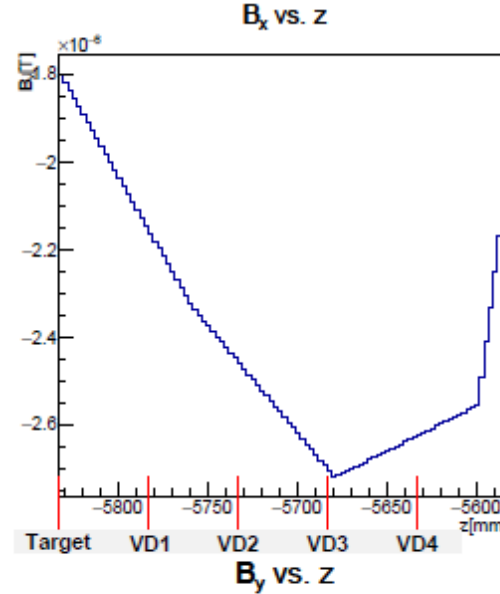
Target OUT



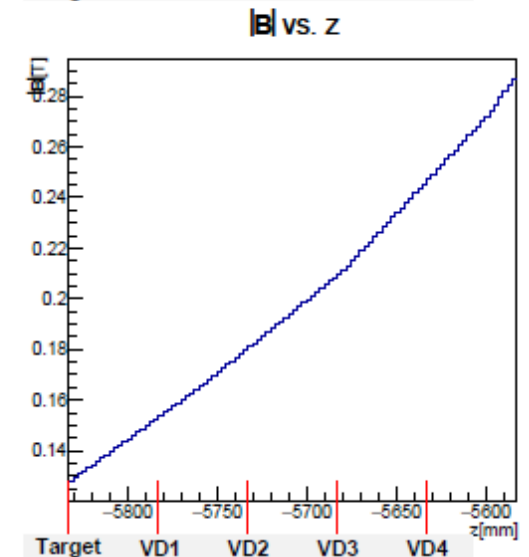
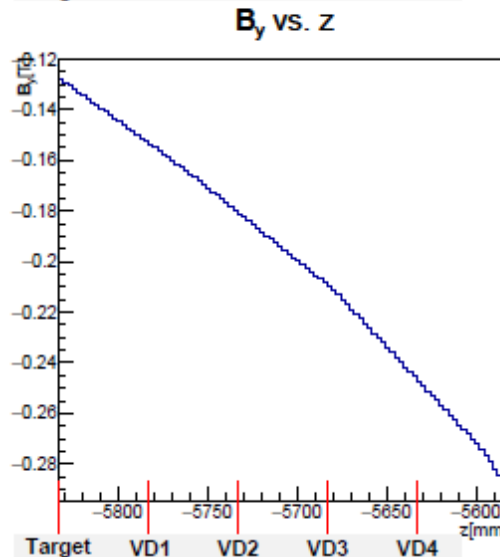
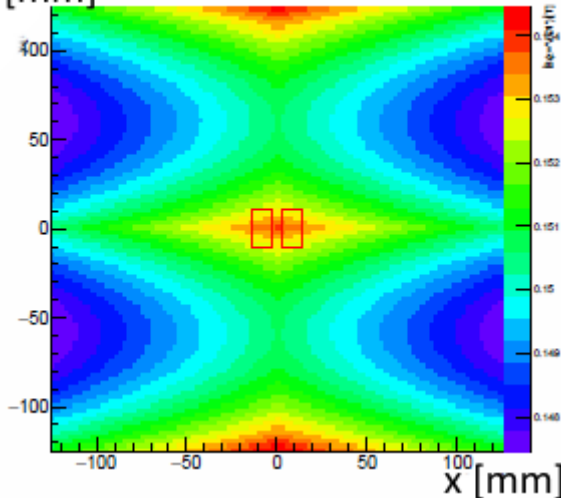
Track reconstruction in Vertex Detector

Magnetic field in VD

- Inhomogeneous magnetic field ($0.13 \pm 0.0025\text{T}$) in the Vertex Detector volume

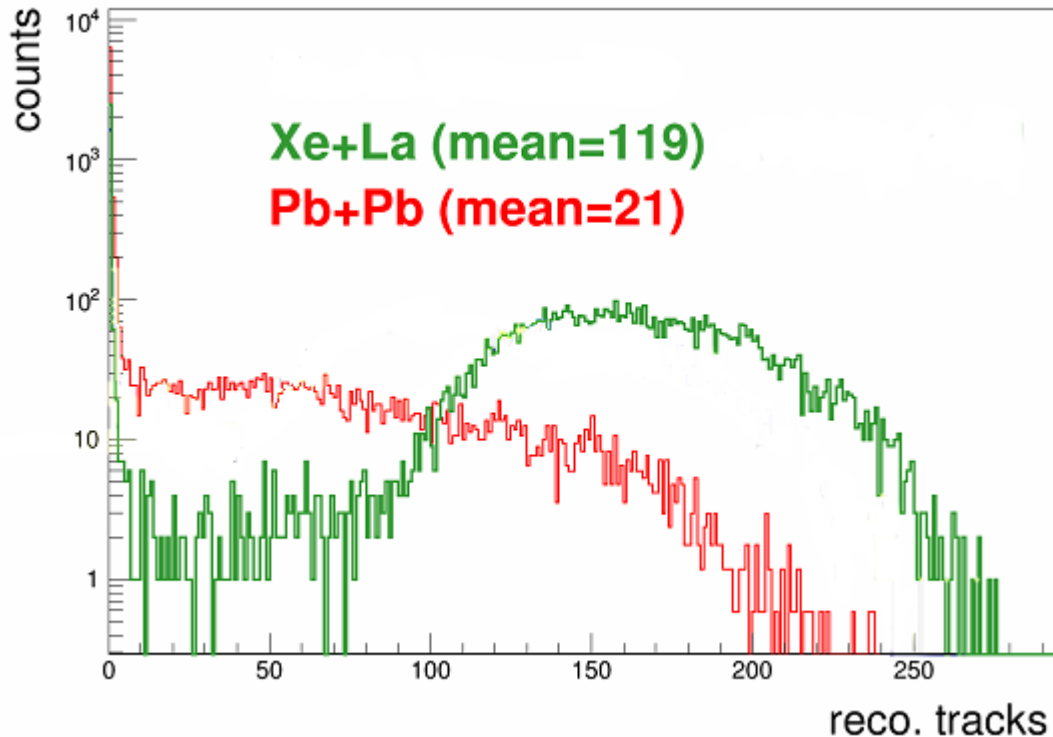


$|B|$ on the 1st station



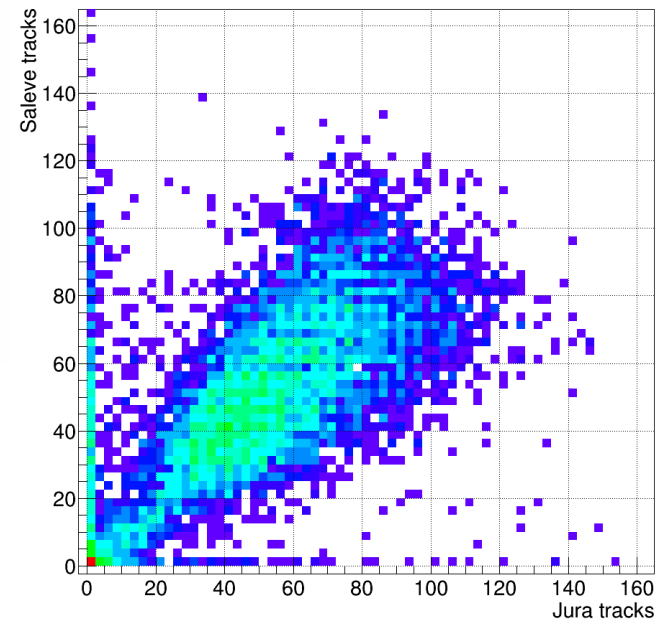
Xe+La data taking

- Track multiplicity

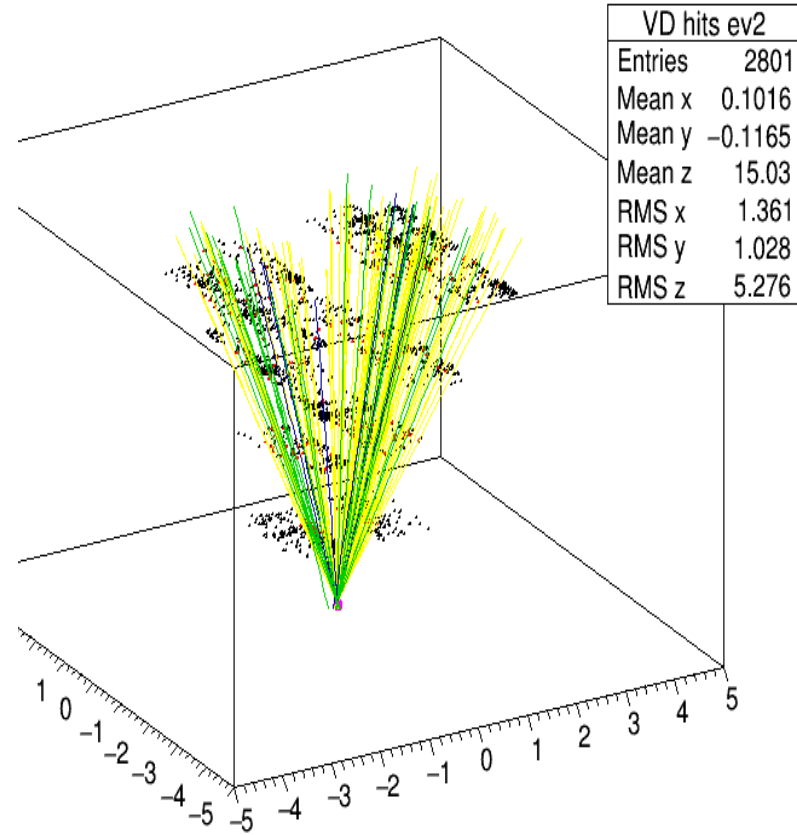
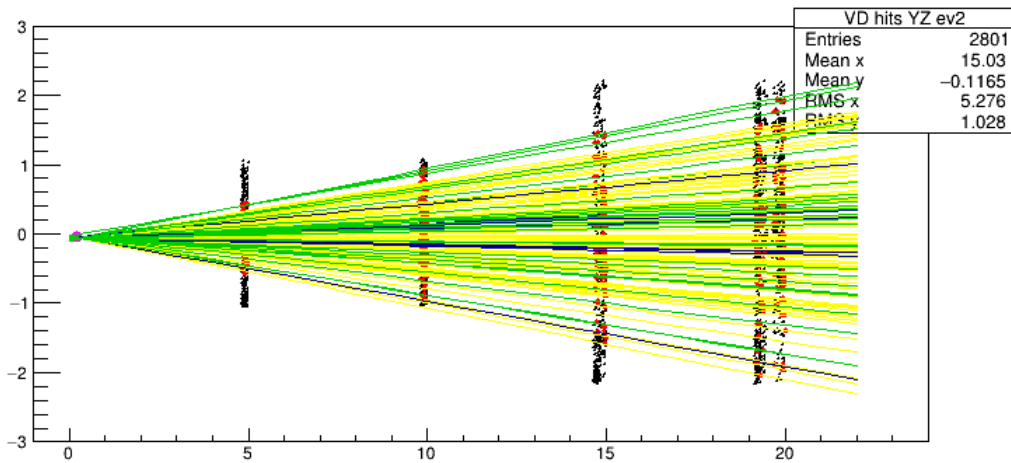
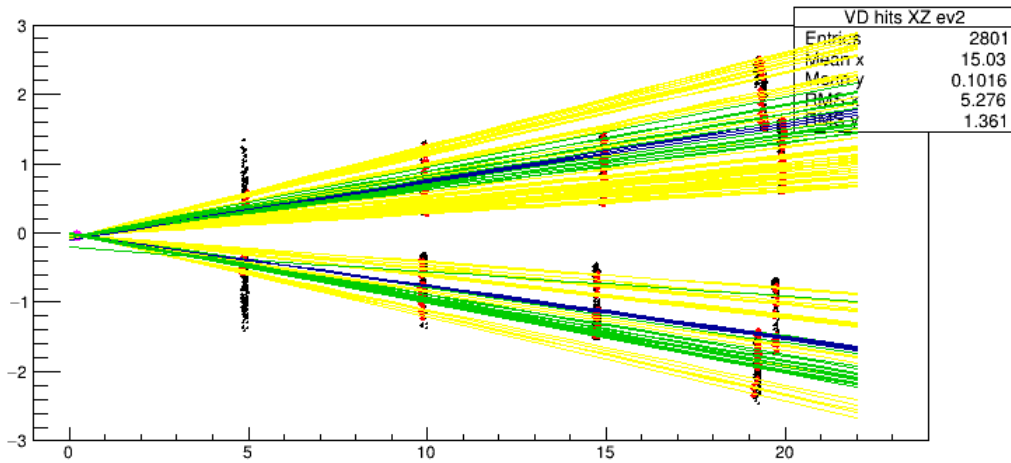


- Pb+Pb ($A = 208, A = 208$)
- Xe+La ($A = 129, A = 139$)

- track correlation



Full event reconstruction

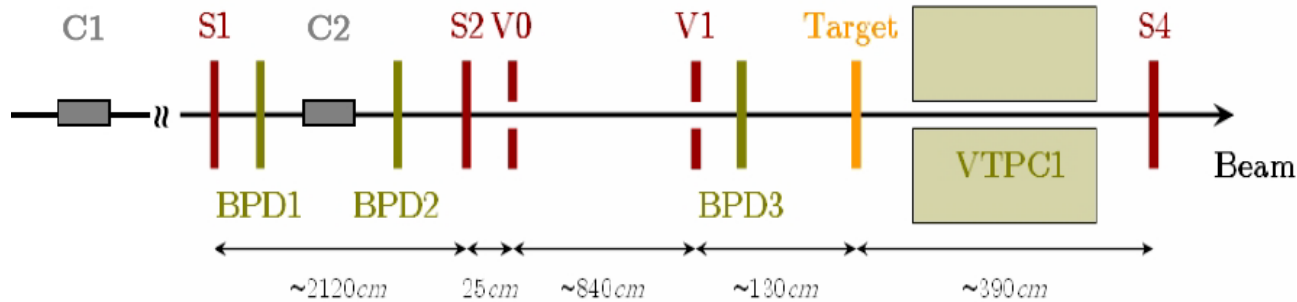


Data taking results

Summary & plans

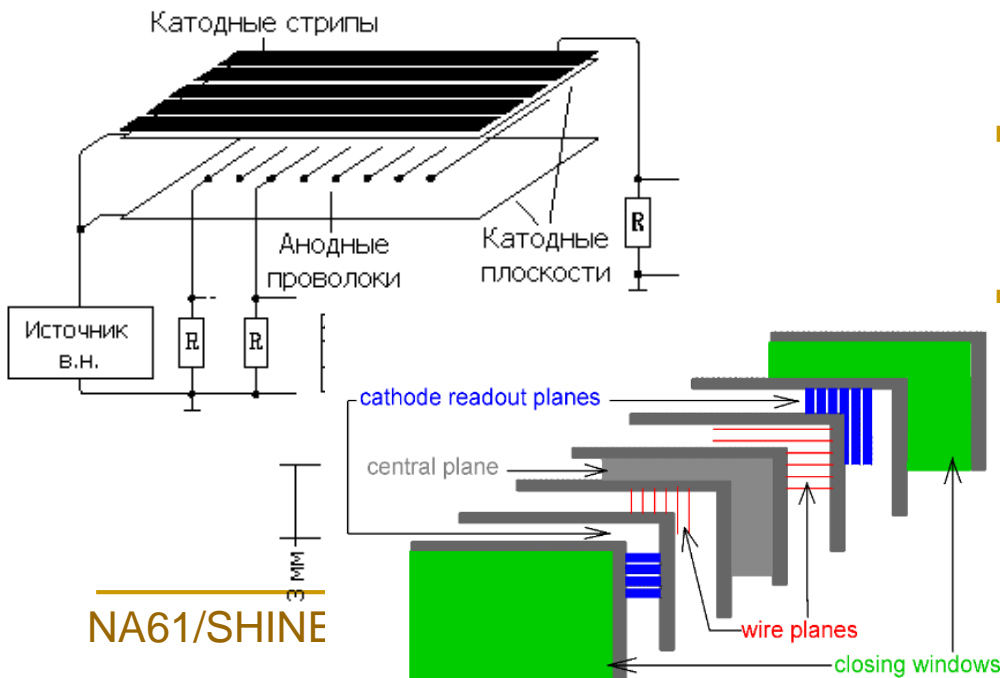
- Data taking with SAVD:
 - 2016 Dec: Pb+Pb at 150A GeV/c
→ **first direct observation of D^0 signal in nucleus-nucleus collisions in fixed target experiment;**
 - 2017 Nov–Dec : Xe + La run at 150A, 75A and 40A GeV/c
→ reconstruction is ongoing;
 - 2018 Nov-Dec: Pb+Pb at 150A GeV/c
Open Charm production beam time;
Expected to collect 10M central events.
- After LS2 high statistic Pb+Pb data taking with upgraded Vertex Detector is proposed in 2021-2023.
- The measurements will provide the long-awaited data crucial for the following topics:
 - J/ψ production as the signal of deconfinement;
 - Open charm yield as signal of deconfinement;
 - Open charm production mechanism: pQCD vs Statistical models.

Beam detectors



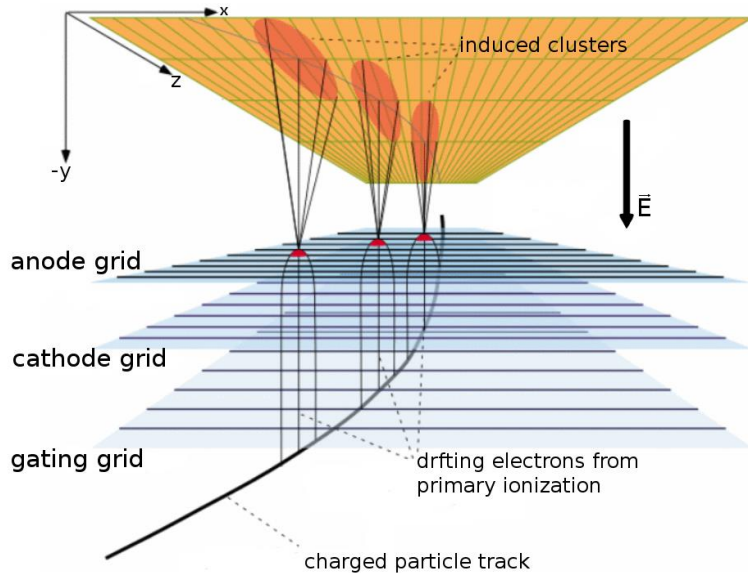
- C1 and C2 –hadron identification,
- S1, S2, V0, V1, BPD1/2/3 -determination projectile trajectory,
- S4 -selection of projectile+target interactions

- Each of three **BPDs (multi-wire proportional chamber)** measures the transverse position of beam particle;
 - Ionizing particle that passes through the chamber will ionize surrounding gaseous atoms;
 - The resulting ions and electrons are accelerated by the electric field, causing a localized cascade of ionization; This collects on the nearest wire (anod) and one reads a signal;
- By computing signals from all the wires, the particle trajectory can be found.

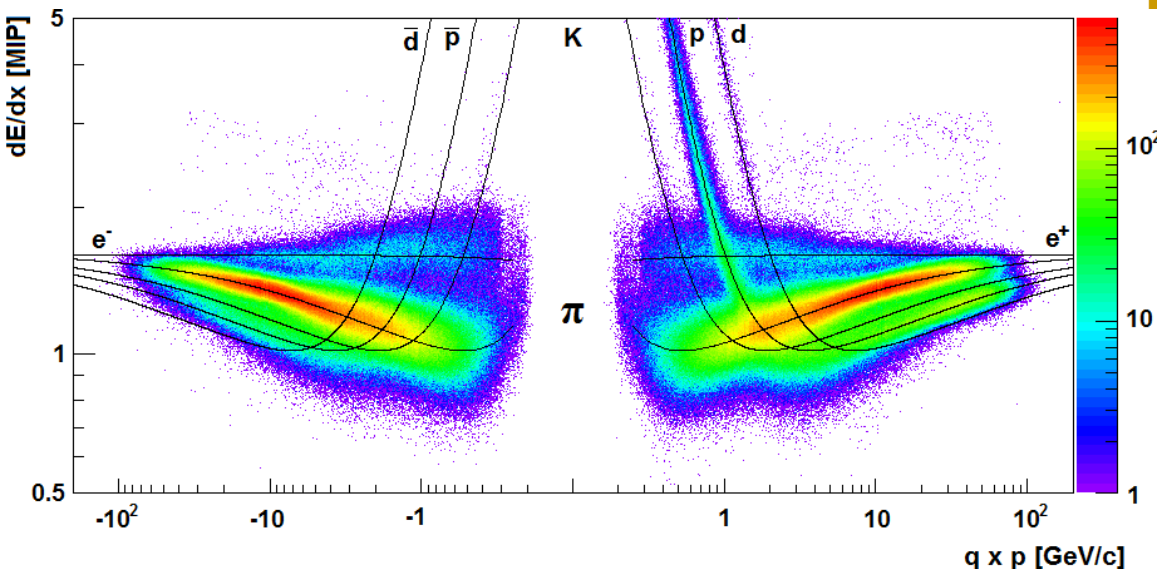


NA61/SHINE

Time-projection chamber (TPC)

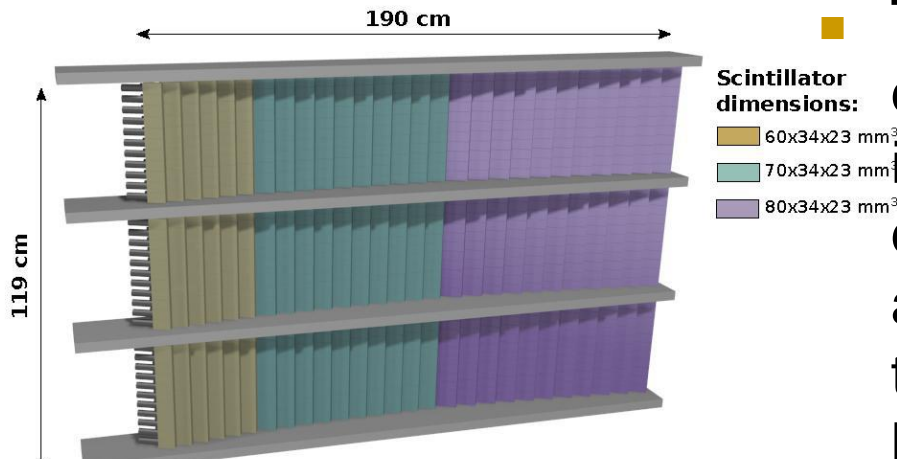


- TPCs consist of a large volume of gas in which particles leave a trail of ionization electrons.
- The electrons drift in the uniform vertical electric field with constant velocity towards the read-out chamber where their arrival time, position, and total amplitude of the signals are measured with proportional wire chambers.

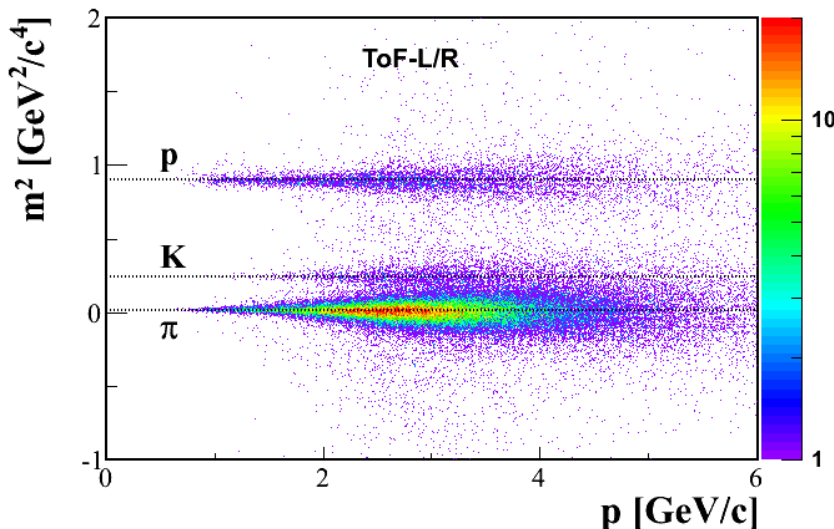


- TPCs provide precise measurements of
 - Electric charge,
 - Momentum and
 - Energy loss dE/dx
 of the produced particles.

Time-of-flight detector (ToF)



- The time of flight of the particle depends upon the start signal that is given by one of the trigger detectors (S1 scintillator counter) and the stop signal produced by the readout of the ToF which was hit by the particle.



$$m^2 = p^2 \left(\frac{c^2 t^2}{l^2} - 1 \right)$$

- It allows for a **mass** measurement in a momentum range not accessible for the TPCs.